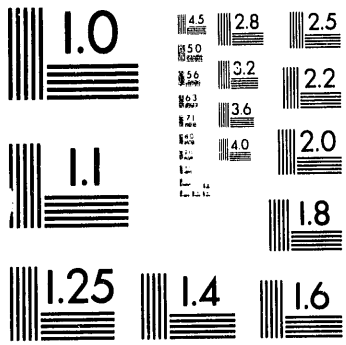
1.0
1.1
1.25
1.4
1.6
1.8
2.0
2.2
2.5
2.8
3.2
3.6
4.0
4.5
5.0
5.6
6.3
7.1

1 of 1

Three-Dimensional Modeling of Diesel Engine Intake Flow, Combustion and Emissions - II

DOE/NASA-Lewis
University of Wisconsin Grant*

December, 1992

Principal Investigators: R.D. Reitz and C.J. Rutland
Engine Research Center
Department of Mechanical Engineering
University of Wisconsin-Madison

*Research sponsored by the U.S. Department of Energy, Assistant Secretary of Conservation and Renewable Energy, Office of Transportation Technologies, administered by NASA-Lewis under Grant number NAG 3-1087, William Wintucky Grant Monitor.

Report Period 10/91 - 12/92

ABSTRACT

A three-dimensional computer code, KIVA, is being modified to include state-of-the-art submodels for diesel engine flow and combustion. Improved and/or new submodels which have already been implemented and previously reported are: wall heat transfer with unsteadiness and compressibility, laminar-turbulent characteristic time combustion with unburned HC and Zeldo'vich NOx, and spray/wall impingement with rebounding and sliding drops. Progress on the implementation of improved spray drop drag and drop breakup models, the formulation and testing of a multistep kinetics ignition model and preliminary soot modeling results are described in this report. In addition, the use of a block structured version of KIVA to model the intake flow process is described. A grid generation scheme has been developed for modeling realistic (complex) engine geometries, and computations have been made of intake flow in the ports and combustion chamber of a two-intake-valve engine. The research also involves the use of the code to assess the effects of subprocesses on diesel engine performance. The accuracy of the predictions is being tested by comparisons with engine experiments. To date, comparisons have been made with measured engine cylinder pressure, temperature and heat flux data, and the model results are in good agreement with the experiments. Work is in progress that will allow validation of in-cylinder flow and soot formation predictions. An engine test facility is described that is being used to provide the needed validation data. Test results have been obtained showing the effect of injection rate and split injections on engine performance and emissions.

CONTENTS

INTRODUCTION

The diesel engine is the leading heavy-duty power plant because of its superior energy efficiency. However, because of environmental concerns, proposed federal emission standards require reductions in both nitric oxides (NOx) and particulates. A detailed understanding of combustion is required in order to work effectively at reducing these by-products of combustion *within* the engine cylinder, while still not compromising engine fuel economy.

The objective of this research program is to develop an analytic design tool for use by the industry to predict engine performance and emissions. It is expected that the use of advanced modeling tools will enable engine development times and costs to be reduced. The three-dimensional computer code, KIVA [1,2] is being used since it is the most developed of available codes. Part of the research involves implementing state-of-the-art submodels into KIVA for spray atomization, drop breakup/coalescence, multi-component fuel vaporization, spray/wall interaction, ignition and combustion, wall heat transfer, unburned HC and NOx formation, soot and radiation, and modeling the intake flow process.

Previous progress has been described by Reitz et al. [3,4], and in a previous Annual Report [5], where it was shown: that adding the effects of unsteadiness and compressibility to the heat transfer submodel improves the accuracy of heat transfer predictions; that drop rebound should be included in spray/wall interaction models since rebound can occur from walls particularly at low impingement velocities (e.g., in cold-starting); that the influence of vaporization on the atomization process should be considered since larger spray drops are formed at the nozzle with vaporization; that a laminar-and-turbulent characteristic time combustion model has the flexibility to match measured engine combustion data over a wide range of operating conditions; and, finally, that the characteristic time combustion model can also be extended to allow predictions of ignition.

The implementation of improved models for the prediction of spray drop drag and breakup, and for modeling ignition and combustion, intake flow and soot formation is described in this report. The research also involves the use of the computer code to assess the effects of subprocesses on diesel engine performance, and the accuracy of the predictions is being tested by comparisons with engine experiments. To date, comparisons have been made with measured engine cylinder pressure, temperature and heat flux data, and the model results are in good agreement with experiments [3, 4, 5].

Work is also in progress that will allow validation of in-cylinder flow and soot formation predictions. An engine test facility is described that has been constructed and is being used to provide the validation data.

Close contact is being maintained with engine industries during the course of the research. This includes participation in DOE diesel engine working group meetings[1]. In addition, technology has been transferred directly to industry (e.g., we have already made FORTRAN code for the ignition subroutine listed in Appendix 3 of this report available to the Software Development Group, Engine Division, Caterpillar Inc. - W. Brown of this group spent the past year at Madison). Two of our graduate students (D. Nehmer and R. Hessel) are now employed by Cummins Engine company and have taken elements of the technology with them to Cummins. We have continued our involvement with the KIVA Users Group (including co-organizing the 2nd International KIVA Users Group Meeting in Detroit on February 23rd, 1992, and producing Newsletters 5, 6 and 7, see Appendix 1). This activity has kept us informed of code enhancements and new developments elsewhere in the international user community.

BACKGROUND OF RESEARCH PROGRAM

The research program was initiated in the Fall of 1989 as a five year program. The emphasis of the research is on the application of a comprehensive engine combustion code to assess the effect of the interacting subprocesses on diesel engine performance, rather than on the development of new models for the subprocesses themselves. The elements of the code are being assembled from existing state-of-the-art submodels. This use of multidimensional modeling as an engine development tool is timely and justifiable due to recent advances in submodel formulations.

The computer model is based on the KIVA-2 and KIVA-3 computer codes that were written at the Los Alamos National Laboratories [1,2] and allow computations of turbulent, multi-phase, combusting 3-D engine flows. The codes solve the conservation equations for the transient dynamics of vaporizing fuel sprays interacting with flowing multicomponent gases which are undergoing mixing, ignition, chemical reactions, and heat transfer. The codes have the ability to calculate flows in engine cylinders with arbitrary shaped piston geometries, and include the effects of turbulence and wall heat transfer.

Many of the in-cylinder processes occur on time and length scales that are too short to be resolved in practical computations. Thus, submodels are needed

[1]Prof. Rutland gave the presentation "Diesel Intake Flow Modeling," Spring 1992 DOE Meeting, Southwest Research Institute, San Antonio, Texas, May 4-5, 1992. Prof. Reitz gave the presentations 'Progress in 3-D Modeling of Diesel Engine Intake Flow, Combustion and Emissions' and "Measurements of the Effect of Injection Rate and Split Injections on Diesel Engine Soot and NOx Emissions" at the Fall 1992 DOE Diesel Group Meeting, Princeton University, November 5-6, 1992.

to describe the processes, and the submodels require detailed validations before they can be used for engine performance predictions (Reitz [6]). For example, for modeling sprays, submodels are needed to describe drop drag, drop turbulence interaction, vaporization, atomization, breakup and coalescence, and spray/wall interaction. These spray processes influence the combustion and pollutant formation processes profoundly through their effect on the fuel-air distribution in the engine.

Individual submodels are usually developed starting from simplified theoretical models or experiments that isolate a particular process. However, the accuracy of predictions made using combinations of submodels to describe the performance of the overall engine must be assessed by comparisons with detailed and informative engine experiments. An important component of the present research is to use engine comparisons to identify areas where submodels need improvement, and to develop improved models where necessary.

The program was expanded to include the modeling of the diesel engine intake process in 1990 due to its importance in the combustion process. In 1991 the research program was expanded again to include engine experiments for the acquisition of validation data. A summary of the 1989-1991 research activities has been described in the 1991 Annual Report, Ref. [5].

The research program has been organized into three main activities: Part A - Submodel Implementation, Part B - Model Application and Part C - Experiments. Progress in the Part A tasks is described on page 7 and in Table 1 below. Part B tasks are described on page 27. The Part C tasks are described on page 29.

Table 1 Status of KIVA Submodels

	Original KIVA	Submodels being implemented/updated	yr
combustion	Arrhenius	laminar-turbulent char time	1-3
unburned HC	Arrhenius	laminar-turbulent char time	1
NOx	Zeldo'vich	Zeldo'vich	1
heat transfer	law-of-the-wall	compressible, unsteady	1-2
wall impinge	none	rebound-slide model	1-2
atomization	Taylor Analogy Breakup	surface-wave-growth	1-3
intake flow	assumed initial flow	KIVA-3 computed intake flow	2-4
ignition	none	Shell multistep model	2-3
vaporization	single component	multicomponent	1-4
soot	none	KIVA-coal	3-4
radiation	none	Rayleigh-limit, band model	3-4

CURRENT PROGRESS

PART A - Submodel Implementation

A summary of the submodels that are being added to KIVA and the time-table for their implementation is given in Table 1. The models include improved models for combustion, unburned HC and NOx, wall heat transfer, spray/wall impingement, atomization, intake flow, ignition, multi-component vaporization, and soot and radiation. Details of the current and projected status of the models are presented in the last column of Table 1.

The research program is currently in its fourth year. Progress to date in each of the Part A tasks scheduled for the third year of the grant is discussed in this section. Additional details of progress are given in Ref. [5]. Appendix 2 gives additional details of published papers connected with the research activities in the past year. Appendix 3 contains a FORTRAN source code listing for the multistep ignition submodel that has been implemented as part of the research.

Improved and/or new submodels which have already been implemented in KIVA have been described by Reitz et al. [3,4], including models for: wall heat transfer with unsteadiness and compressibility, laminar-turbulent characteristic time combustion with unburned HC and Zeldo'vich NOx, and spray/wall impingement with rebounding and sliding drops. In addition, progress on intake flow modeling, including the generation of grids for computations in realistic manifold geometries, and the use of an block structured mesh version of KIVA, KIVA-3, have been described by Reitz et al. [4].

Results to date show that adding the effects of unsteadiness and compressibility improves the accuracy of the heat transfer predictions; spray drop rebound can occur from walls at low impingement velocities (e.g., in cold-starting); and that a laminar-and-turbulent characteristic time combustion model has the flexibility to match engine combustion data over a wide range of operating conditions. Continued progress on intake flow modeling, and on diesel spray atomization and ignition/combustion and emissions models is described next.

ATOMIZATION AND DROP DRAG - As noted by Reitz et al. [4], vaporizing spray computations have been found to be very sensitive to numerical parameters, especially to the grid size near the exit of nozzle. This motivated re-examination of the parameters of the atomization model since the atomization process occurs mostly near the nozzle exit. For this purpose, comparisons have been made by Liu et al. [7] with drop breakup, velocity and trajectory measurements of Liu and Reitz [8].

The experiments consisted of a Berglund-Liu drop generator and an air jet nozzle, arranged in a cross-flow pattern so that the drops are suddenly exposed to the air as in Fig. 1. Drop sizes were measured with a Phase Doppler Particle Analyzer [8]. This experimental configuration is useful because the relatively low liquid and spray drop density does not favor collisions and coalescences of the drops which complicate the interpretation of typical diesel spray experiments. Drop breakup was modeled using both the wave instability model (Reitz [9]) that has benn used in our diesel engine combustion simulations, and the standard KIVA TAB breakup model [10]. The breakup models contain model constants that were also evaluated as part of the present study.

The computations shown in Fig. 1 were made on a 3-D mesh of 32x16x84 cells in the radial, azimuthal and axial directions, respectively. Figure 1 shows computed drop locations and gas velocity vectors in the plane of the nozzle, 4 ms after the start of the injection for a case with an air velocity of 100 m/s at the air nozzle exit.

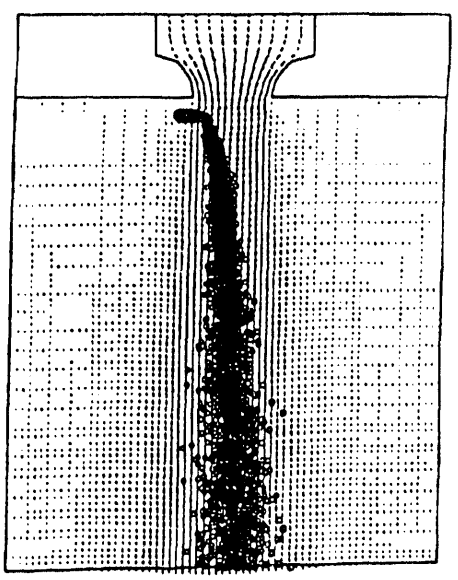

Fig. 1 Computed drop locations and gas velocity vectors 4 ms after the start of injection for air jet velocity of 100 m/s. Stream of 170 μm diameter drops enters air jet from the left at 16 m/s.

Measured and predicted (parent or outermost) drop trajectories are compared in Fig. 2. In this figure the drops enter from the left (at X=Y=0), and the measured data is indicated by squares. Figure 2 shows that good agreement with the measured trajectories can be obtained when a modified drag coefficient is used that accounts for the fact that the parent drops are deformed by the gas flow as they breakup. The drop deformation is modeled dynamically as a function of the local flow conditions around each drop [7].

The corresponding predicted drop size variation across the air jet using the two different breakup models is shown in Fig. 3. In the wave instability model (Wave [9]), drop breakup times and breakup sizes are assumed to be proportional to wave growth rates and wavelengths obtained from a stability analysis of liquid jets. The final (stable) drop size reached by drops that penetrate all the way through and emerge from the other side of the air jet are seen to be in good agreement with the measured drop size at the jet edge in Fig. 3. Figure 3 also shows computations made with the standard KIVA TAB breakup model [10]. The TAB model final drop size prediction is seen to under estimate the measured drop size significantly.

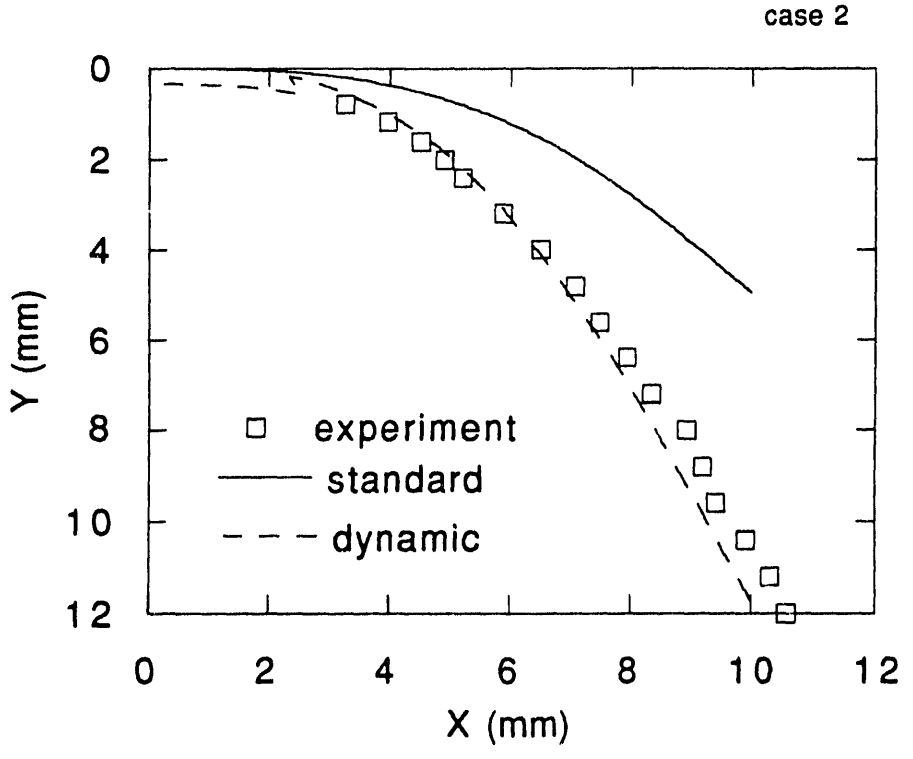

Fig. 2 Comparison of wave breakup model predictions and measured drop trajectory for air jet velocity 59 m/s. Solid line - standard drop drag, dashed line - dynamic drag model that accounts for drop distortion effects.

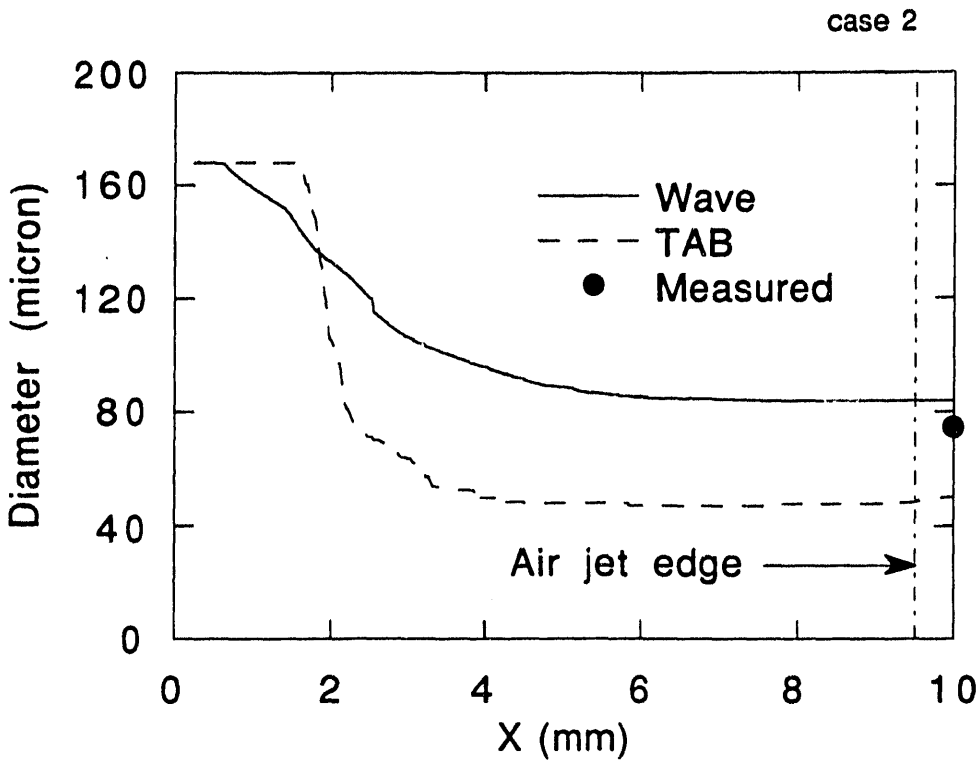

Fig. 3 Predicted drop Sauter mean diameter variation with distance across the jet for air jet velocity 59 m/s using the wave (solid line) and TAB (dashed line) models. Solid circle shows PDPA measured drop diameter outside air jet.

The effect of the sensitivity of drop trajectories to drop drag coefficients observed in Fig. 2 for single drops was also assessed for diesel-type sprays [7]. The results show that spray-tip penetration is quite insensitive to the value of the drop drag coefficient. This somewhat surprising result was found to be due to the fact that changes in the drag coefficient produce changes in the drop-gas relative velocity which, in turn, cause changes in the spray drop size through the drop breakup and coalescence processes. The changes occur in such a way that the net effect on the spray tip penetration is small over the range of tested conditions. However, the results indicate that the drag model does influence the spray drop sizes, and this has an important effect on fuel-air mixing since spray vaporization rates depend strongly on the drop size.

IGNITION AND COMBUSTION MODELS - The ignition delay is an important parameter in the operation of diesel engines since it influences hydrocarbon and NO_x emissions. During the delay period, the injected fuel undergoes complex physical and chemical processes such as atomization, evaporation, mixing and preliminary chemical reaction. Ignition takes place after the preparation, and reaction of the fuel-air mixture leads to fast exothermic reaction. Approaches to describe autoignition phenomena in diesel engines in multi-dimensional models have been reviewed by Kong and Reitz [11].

The kinetics chemistry submodel used for ignition and combustion modeling in the standard KIVA considers a single step Arrhenius mechanism for the stoichiometric reaction of the fuel. Kong et al. [12] used the Arrhenius model to describe ignition together with a laminar and turbulent characteristic time model for combustion. The latter model has been used successfully in spark-ignited engine studies and for premixed- and fuel-injected two-stroke engines (Reitz [13] and Kuo and Reitz [14, 15]). In this way the combustion model has been extended to allow predictions of ignition. Kong et al. [12] found that it was possible to match homogeneous-charge, compression-ignition engine experiments reasonably well with one set of model constants.

A more accurate prediction of ignition has been achieved by implementing the multistep Shell kinetics model of Halstead et al. [16, 17] in KIVA. The implementation details of the model are given in Appendix 3 of this report. Figure 4 shows a comparison between spray ignition experiments and KIVA computations of ignition using the Shell model. The experiments were conducted in a constant volume bomb at the Sandia Labs (Edwards et al. [18]), and used diesel fuel (simulated in the computations as Hexadecane) injected into compressed air at 30 atmospheres and 1070 K. Ignition is seen in Fig. 4 to have occurred by 1.13 ms after the beginning of the injection, as represented by a luminous zone located at the edge of the spray, some distance downstream of the nozzle. By 1.51 ms the luminous zone extends over most of the spray, indicating that combustion has commenced.

The predicted temperature contours are also shown in Fig. 4 for comparison, and it is seen that the location and timing of the ignition process is predicted fairly well by the model. Similar good levels of agreement between measured and predicted ignition delay times were also found for other chamber gas temperatures as shown in Fig. 5.

Figure 6 shows results of comparisons of measured engine cylinder pressure data of Yan and Borman [19] in a Cummins NH engine operated under the conditions given in Table 2. The predictions were made using the standard Arrhenius and the multistep Shell ignition models. Post-ignition combustion was simulated using the single-step Arrhenius model in both cases. The single-step kinetics model is seen to work reasonably well.

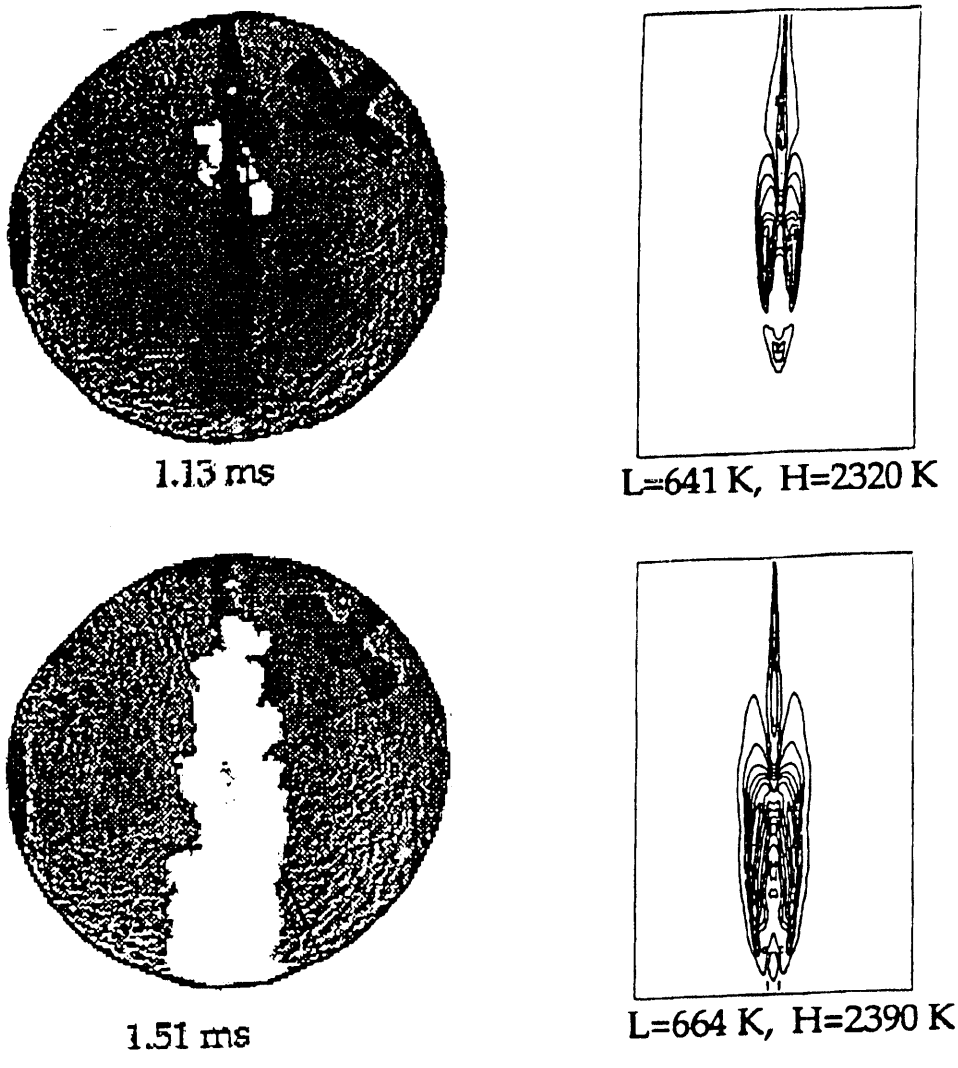

Fig 4. Comparison of measured and predicted spray ignition data for the Sandia constant volume bomb experiments [17].

However, it was found necessary to use a different combustion (pre-exponential) model constant than that used for computations with the Caterpillar engine (see later Fig. 15), indicating that the single-step Arrhenius model is not predictive.

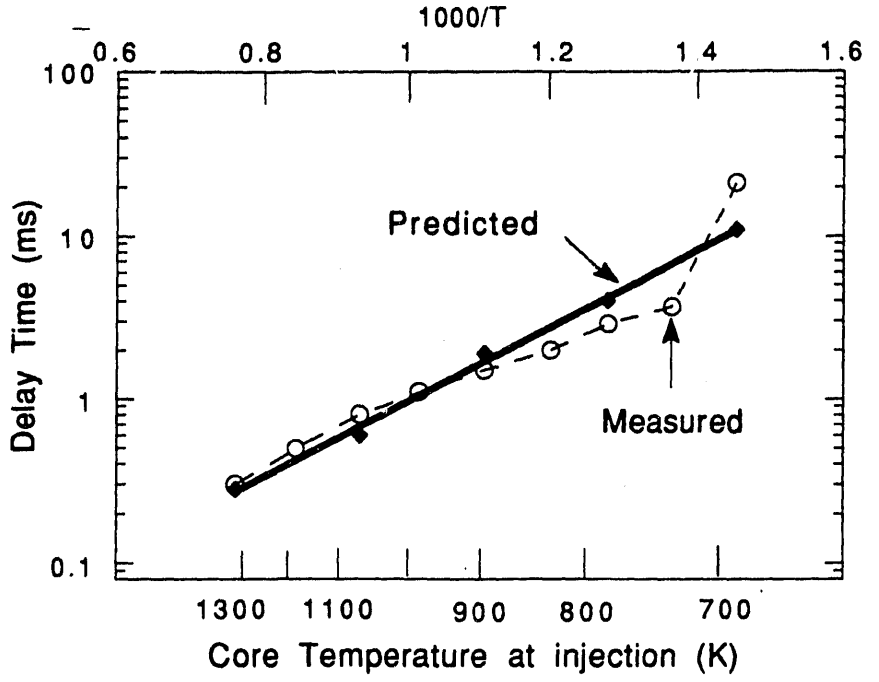

Fig 5. Comparison of measured and predicted ignition delay times for ignition for the Sandia constant volume bomb at different chamber gas temperatures.

Table 2 Cummins Engine Data

Cylinder Bore	139.7 mm
Stroke	152.4 mm
Compression ratio	13.23
Displacement	2.33 liters
Number of spray nozzle orifices	8
Nozzle hole diameter	0.2 mm
Engine speed	1500 r/min (constant)
Overall equivalence ratio	0.6
Air flow rate	0.353e-2 kg/cycle
Fuel flow rate	0.144e-3 kg/cycle
Intake tank pressure	148.2 kPa
Intake tank temperature	302 K
Cylinder wall temp	405 K
Cylinder head	486 K
Piston surface	578 K
Mass average gas temperature at IVC	359 K
Cylinder pressure at IVC	157.9 kPa
Swirl number	1.0
Fuel	Tetradecane
Injection starts	18º BTDC
Injection ends	11º ATDC

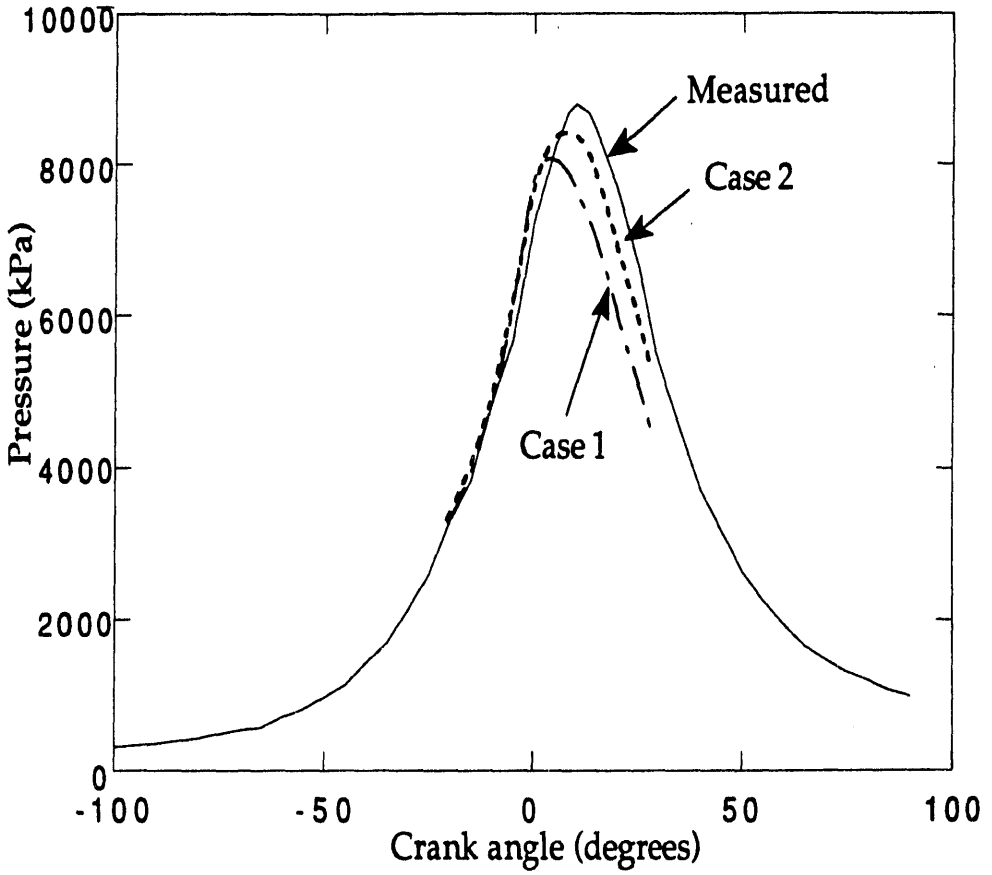

Fig. 6 Measured and predicted pressure histories with the standard one-step Arrhenius model (Case 1) and the multistep Shell ignition model (Case 2). Cummins engine at 1500 rev/min.

The multistep ignition model is more predictive. The computations of Fig. 6 used parameters derived from out-of-engine, low temperature chemistry data, and the multistep model is seen to give excellent results prior to the main stage of combustion.

Details of the predicted location and time-history of the ignition process are summarized in Fig. 7. Fuel injection starts at 18 degrees BTDC. Ignition takes place some distance downstream of the nozzle at the spray edge at about 9 degrees BTDC. This is evidenced by the high temperature contours which are seen to surround the spray in this region in Fig. 7, consistent with the constant volume bomb experimental ignition results of Fig. 4. The build-up and subsequent rapid consumption of the intermediate, branching and radical species that control the ignition process are shown as a function of crank angle in the ignition cell in the inset plot. After the ignition, the gas temperature variation in the ignition cell reflects the balance between the energy released due to combustion and the energy required to vaporize the liquid fuel.

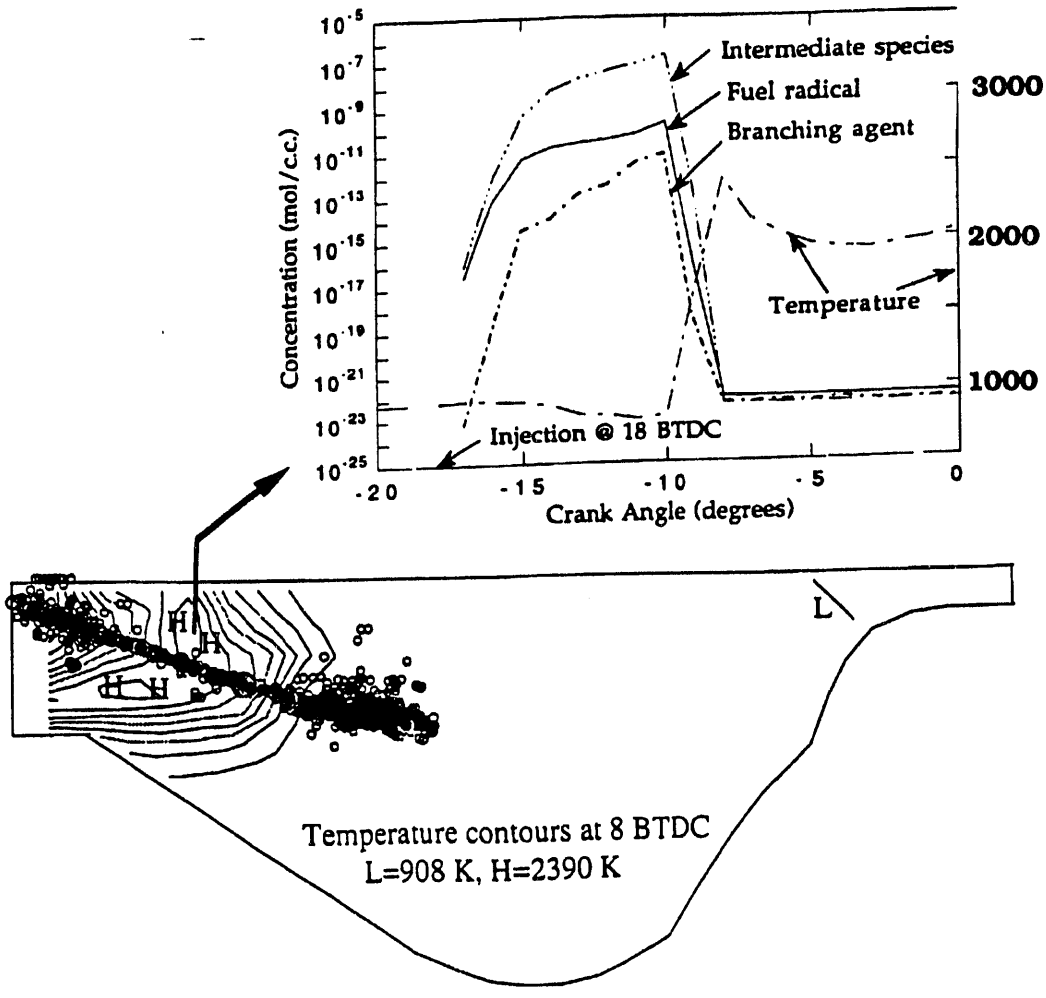

Fig. 7 Predicted spray drop locations and temperature contours in the Cummins engine at 8 degrees BTDC. Inset plot shows variation of gas temperature and ignition species concentrations with crank angle in the ignition cell.

The discrepancy between the predictions of both the standard Arrhenius and the multistep kinetics models and the measured results after ignition suggests the need to consider other effects such as turbulent mixing on post-ignition combustion. Also, discrepancies with measured data have been found to be influenced by numerical errors, and by the details of the fuel injection parameters by Reitz et al. [4]. Further investigation of these effects is in progress.

SOOT AND NOX MODELS - As described in the previous annual report, the extended Zeldo'vich NOx model [20] has also been implemented in KIVA. Two soot formation models have been implemented into KIVA in the current activity. The first is the Surovkin model [21] which had previously been implemented by Gentry et al. [22] in the KIVA-COAL code (for coal-slurry combustion modeling). The second is the simpler Hiroyasu model which is a two equation model for the soot mass formation rate and the soot mass oxidation rate and has been implemented in KIVA by Bertoli et al. [23].

In the Surovkin model the soot formation process starts by considering the formation of radical nuclei which grow to become soot particles by surface growth and agglomeration mechanisms. The model consists of 5 simultaneous rate equations for radicals, radical size, particles, particle size, and a hydrocarbon consumption term. The soot particles themselves are subject to oxidation processes following the Nagle and Strickland-Constable mechanism [24]. In the present implementation the equations were solved using the Runge-Kutta approach, since the original explicit method of Ref. [22] was found not to work in the high fuel concentration and high temperature environment of the diesel engine.

The results given in Fig. 8 show predictions of the thermal decomposition of C6H6 in an inert high temperature environment, and the results agree well with the model results of Surovkin [21] (not shown). However, detailed investigations of the results suggest that the soot particle size model needs further development, especially for engine applications, since the model can produce more soot mass than the original fuel has available. Although the Surovkin model has been used in engine computations (see Fig. 9), it is believed that the model over-predicts the soot mass. One possible solution would be to modify the model constants.

Preliminary calculations with the Hiroyasu model indicate that this model computes soot mass quantities which are in the known engine range. Although this model was not developed for modeling the thermal decomposition of a hydrocarbon fuel, results obtained using the model to compute the soot mass for the thermal decomposition of C6H6 in the absence of oxygen are compared with the Surovkin model in Fig. 8. The Hiroyasu model predicts soot mass levels that are about two orders of magnitude lower than those from the Surovkin Model.

Thus it is expected that the Hiroyasu model will work well in the engine environment, but the Surovkin model, originally developed for thermal decomposition, will require additional work to be useful for engine computations.

Nevertheless, the results in Fig. 9 show predicted temperature, NOx and soot particle distribution contours obtained using the Surovkin model in the

Cummins engine at 6 degrees BTDC. The temperature data indicates that a combustion region surrounds the spray near the nozzle ('h' identifies the high contour location). The NOx contours reveal that the NOx concentrations are highest in region where the gas temperatures are the highest, as expected from the sensitivity of the NOx reaction mechanism to temperature. The soot particle size contours indicate that the soot concentrations are largest in the colder regions near the spray tip. It is worth noting that soot and NOx are predicted to be formed in different regions of the combustion chamber. This observation is important in developing an understanding of the well-known soot-NOx trade-off.

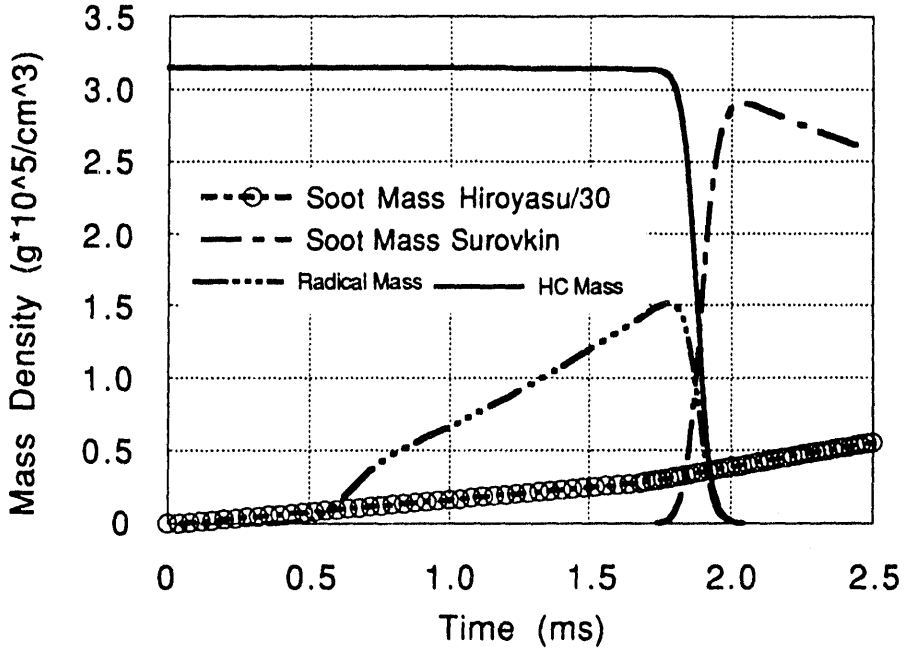

Fig. 8 Comparison of Hiroyasu and Surovkin soot models for the high temperature thermal decomposition of C6H6 in the absence of oxygen.

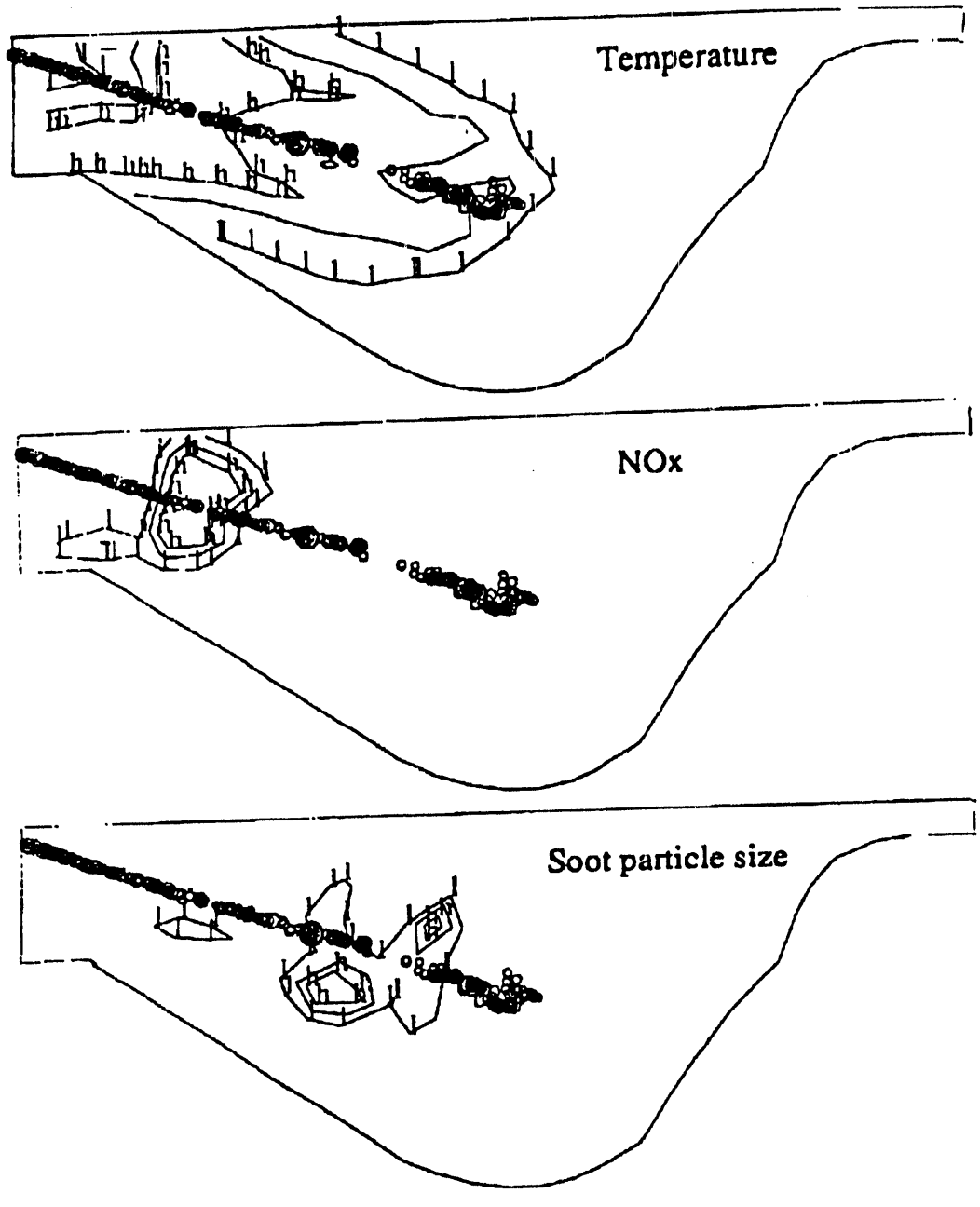

Fig. 9 Predicted gas temperature, NOx and soot particle size distributions in the Cummins engine at 6.5 degrees BTDC. Engine speed 1500 rev/min.

INTAKE FLOW MODELING - Significant advances have been made in intake flow modeling. A methodology has been established by Rutland et al. [25] for generating a realistic grid for the complex geometry of the intake port on the Caterpillar head as shown in Fig. 10.

Creation of the grid required a digitized representation of the geometry. Next, the geometry was imported into the GRIDGEN code of Steinbrenner et al. [26]. Several tools were developed as part of the grid creation process, including a reshaping technique where two or more initial grids are created, each with some aspects desired in the final grid. The result is a composite grid that has the required characteristics, and is much simpler than what could be achieved with GRIDGEN alone [25]. A grid management code was created to help transfer the GRIDGEN grids to KIVA-3. The reshaping techniques are implemented in this program along with the ability to manipulate grid blocks and boundary conditions. The output from this program is run through a modified version of the KIVA grid generation program, K3PREP. In K3PREP the grid generation is disabled but the cell and vertex flags required by KIVA are initialized.

Computations have been made for steady flow (fixed valve lift) in the port, across the two-intake valves and into the cylinder. Pathlines showing predictions of the mixing and flow structures that are setup in the cylinder are shown in Fig. 11. The pathlines are obtained using 'particle' tracks in an instantaneous velocity field. It can be seen that the flow structures change through the cylinder and are not readily described by single parameters such as swirl or tumble ratios.

The steady intake flow computational results have also been compared with experimental mass flow measurements obtained using a SuperFlow 600 flow bench. The calculations were made by specifying the inlet and outlet pressures and calculating the mass flow rates at steady state. The results in Table 3 show that there is reasonably good agreement between the calculated and experimental mass flow rate results.

Table 3. Comparison of mass flow rates from experimental flow bench and KIVA-3 results.

Case	Experiment*	KIVA-3	% Difference
1	37.68**	40.69	-7.99
2	54.17	52.00	+4.01
3	45.96	45.24	+1.57
4	62.33	57.16	+8.29

* mass flow rate in(g/sec)
**accuracy estimated as +/- 8% due to leakage

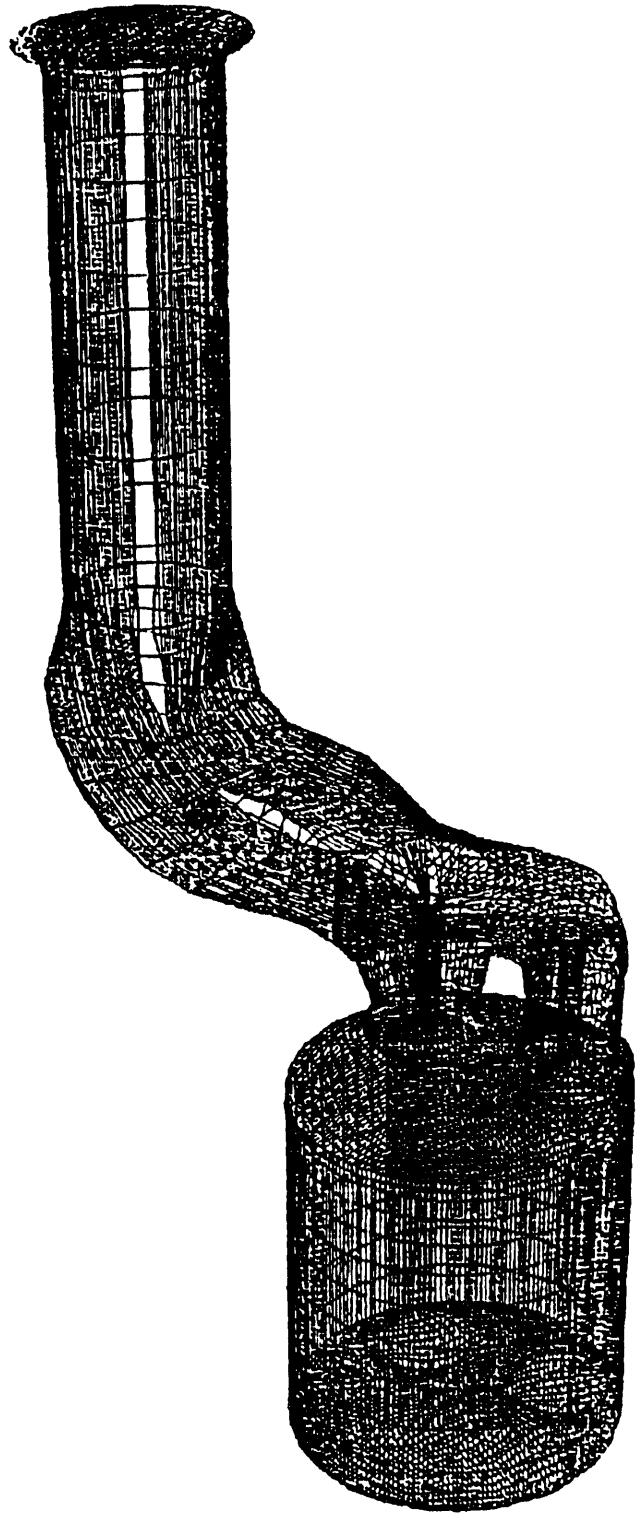

Fig. 10 Computational grid used for the two-intake valve Caterpillar engine. The bell-mouthed entrance to the intake manifold is at the intake surge tank.

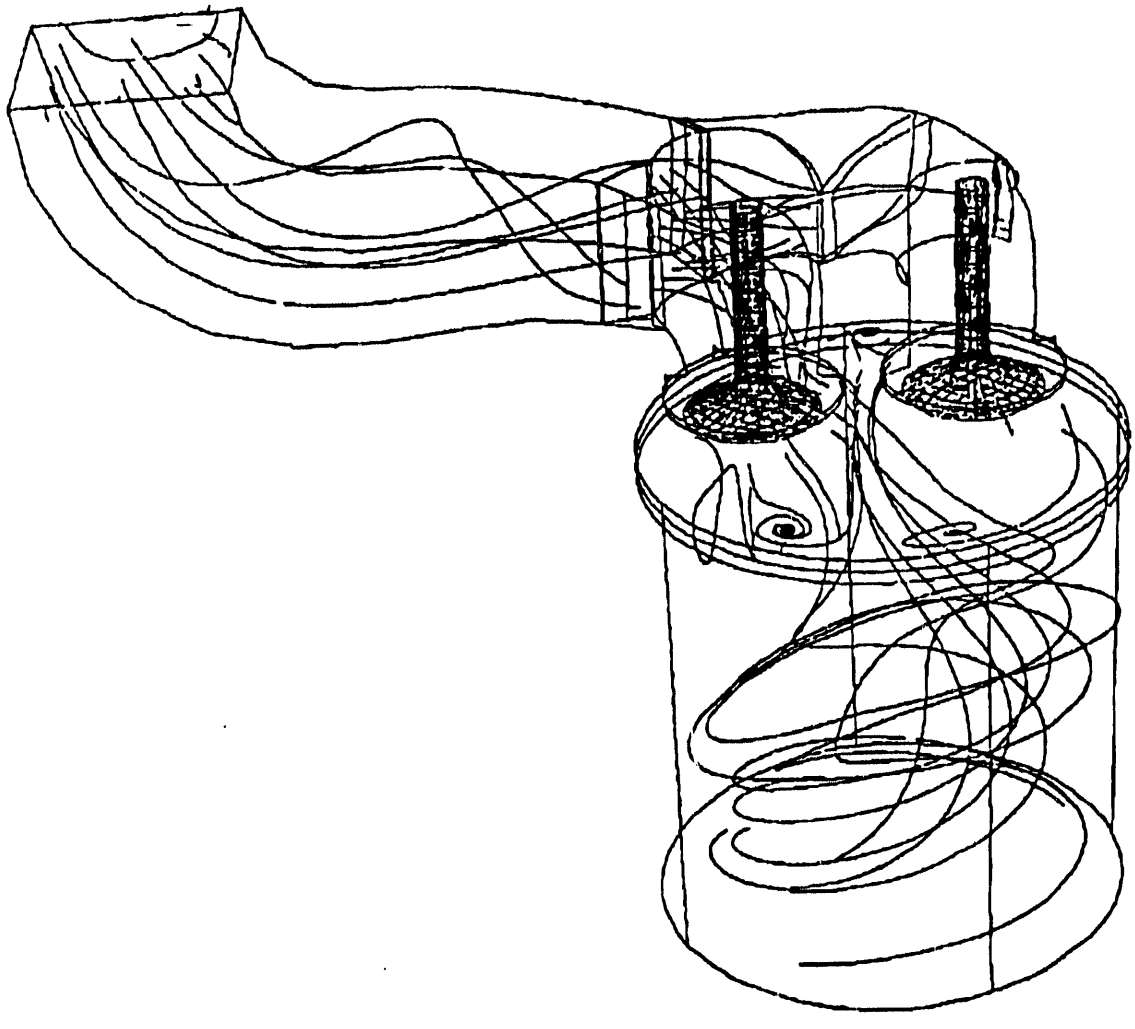

Fig. 11 Predicted in-cylinder fluid pathlines for steady intake flow in the Caterpillar engine.

The capability to accurately simulate moving valves has also recently been implemented. This work takes advantage of the block structured gridding and the 'snapper' algorithm of KIVA-3 [2]. The implementation of the snapper algorithm was described previously by Reitz et al. [4] and it permits regions of the grid to move relative to each other. Grid point connectivity is maintained by periodically regridding or snapping. Adapting the algorithm for use around the valves has proven to be very successful. It is computationally efficient, accurate, and there is no distortion of the physical surfaces.

In addition, a method for closing the valves has been developed. The contact between the valve and the seat is a region rather than a point. This can result in severe time step limitations and difficulty in dealing with the trapped mass since the cell volumes go to zero. The problem has been overcome by using walls to block the flow. The walls are erected when the flow rate across the valves is nearly zero, but before the valve actually touches the valve seat. The inaccuracies introduced are negligible because the flow rates are so low. This approach avoids problems with time step limitations and mass conservation.

Computations have been made with dual moving and closing valves. The valves move according to individual, specified lift profiles. A constant pressure boundary condition was used at the top of the port at the intake surge tank. Results from a sample calculation are shown in Fig. 12 and the run conditions are shown in Table 4. Fig. 12 shows the velocity field on a vertical diametral plane that passes through one of the valves.

A piston with a bowl was added to the grid as shown in Fig. 12. This required some modification of the combustion chamber grid so that it would conform to the shape of the bowl. This modification also required some changes to the grid around the valve curtain region. These changes were implemented fairly rapidly using the capability of GRIDGEN to incorporate an existing grid as a geometry database.

The intake valves open at 8.5 degrees before top dead center. The velocity vector results in Fig. 12 at 0 degrees (TDC) show that fluid flows back into the intake manifold initially as the valves begin to open. By 60 degrees ATDC the piston is moving downward and strong intake flow jets across the valves create large scale vortical flow patterns in the engine.

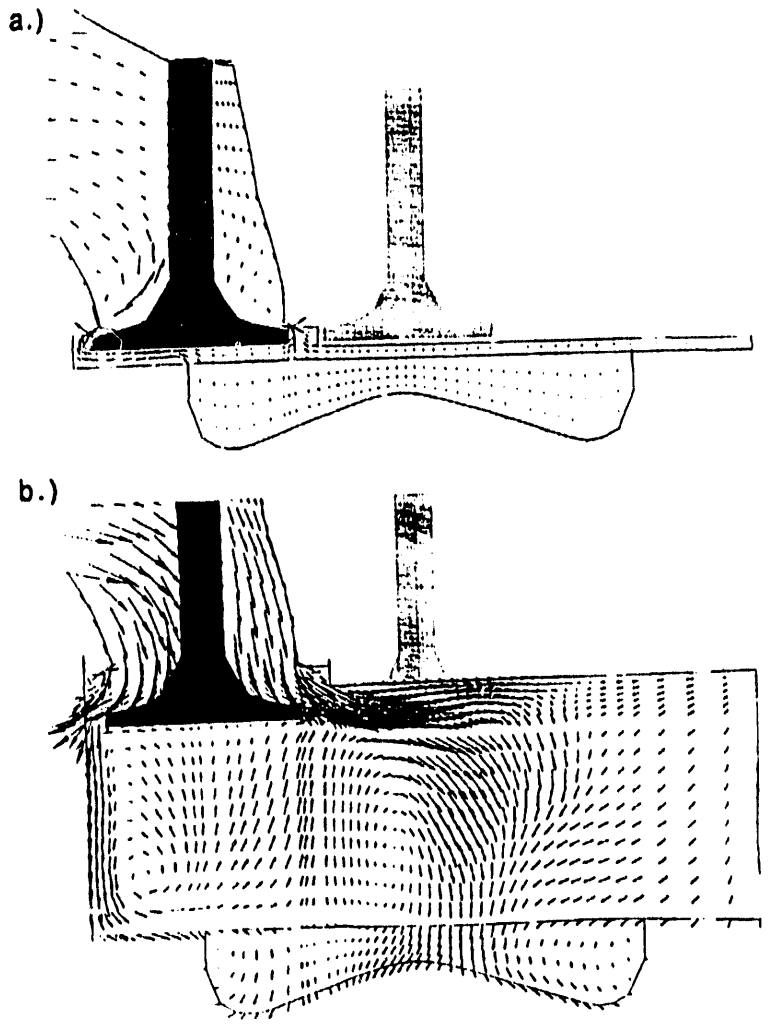

Fig. 12 Velocity vectors in a diametrical plane through one intake valve during the intake stroke for dual moving valves implemented in KIVA-3; (a) 0 degrees (TDC) (b) 60 degrees ATDC. Caterpillar engine 1600 rev/min.

Table 4 Parameters for the unsteady intake flow calculations

Engine R.P.M.	1600
Calculation crank angles	10^0 BTDC to 335^0 ATDC
Intake valve opening	8.5^0 BTDC
Intake valve closing	184^0 ATDC
Initial pressure (port and chamber)	179 KPa
Initial temperature	723 K
Initial turbulent kinetic energy	3.7 m^2/s^2
Boost pressure at inlet boundary	184 KPa

Volume averaged flow quantities as a function of crank angle are presented in Fig. 13. The turbulent kinetic energy is seen in Fig. 13a to increase as the intake flow jets create regions of high production. However, the total turbulence levels begin to decrease even before the intake valves close. By the time of fuel injection the average turbulence level has decayed by an order of magnitude from the peak value.

The volume averaged turbulence integral length scale also increase during the intake process as shown in Fig. 13b. However, this lags the turbulent kinetic energy and peaks around the time of intake valve closing. This lag is consistent with turbulence being created at smaller scales (in the shear layers of the intake jets) and decaying into larger scales as production diminishes. The turbulence length scale also decreases significantly by the time of injection.

The volume averaged swirl ratio is presented in Fig. 13c. The swirl ratio is the average angular velocity of the fluid normalized by the engine r.p.m. with negative values indicating clockwise rotation. The magnitude of swirl increases during intake, decreases slightly before intake valve closing and remains nearly constant for the rest of the compression calculation.

Since the steady flow calculations indicated that a global swirl parameter does not provide an adequate means of assessing intake flow structures, more detailed information about the swirl is of interest. Figure 14 shows swirl profiles averaged over horizontal planes, and plotted as a function of vertical position in the chamber and crank angle. In these figures the piston face is indicated by an arrow. Non-zero swirl below the piston face occurs in the piston bowl.

The plots in Fig. 14 show the rapid increase of swirl during intake. However, most of the increase is located close to the piston face. This is consistent with the findings of the steady flow calculations (Fig. 11). The flow from the intake jets creates localized vortical structures and prevents a chamber-wide structure from forming near the head. Close to the piston face, there is no interference from the valve flow and the flow is constrained to lie in a horizontal plane.

The vertical distribution of swirl can be compared to the volume averaged values in Fig. 13c to show how it changes with time. This is indicated in Table 5 in which the peak swirl magnitudes are compared to the volume averaged magnitudes. The ratio of peak to mean value diminishes from 3.6 near the end of intake valve closing to 1.5 at start of injection. The large ratio near intake value closing is due in part to swirl in the upper part of the chamber that is in an opposite direction from the predominate swirl direction lower in the chamber. The magnitude of this opposite swirl is not large but it occurs over a large region and results in a lower mean magnitude. As the

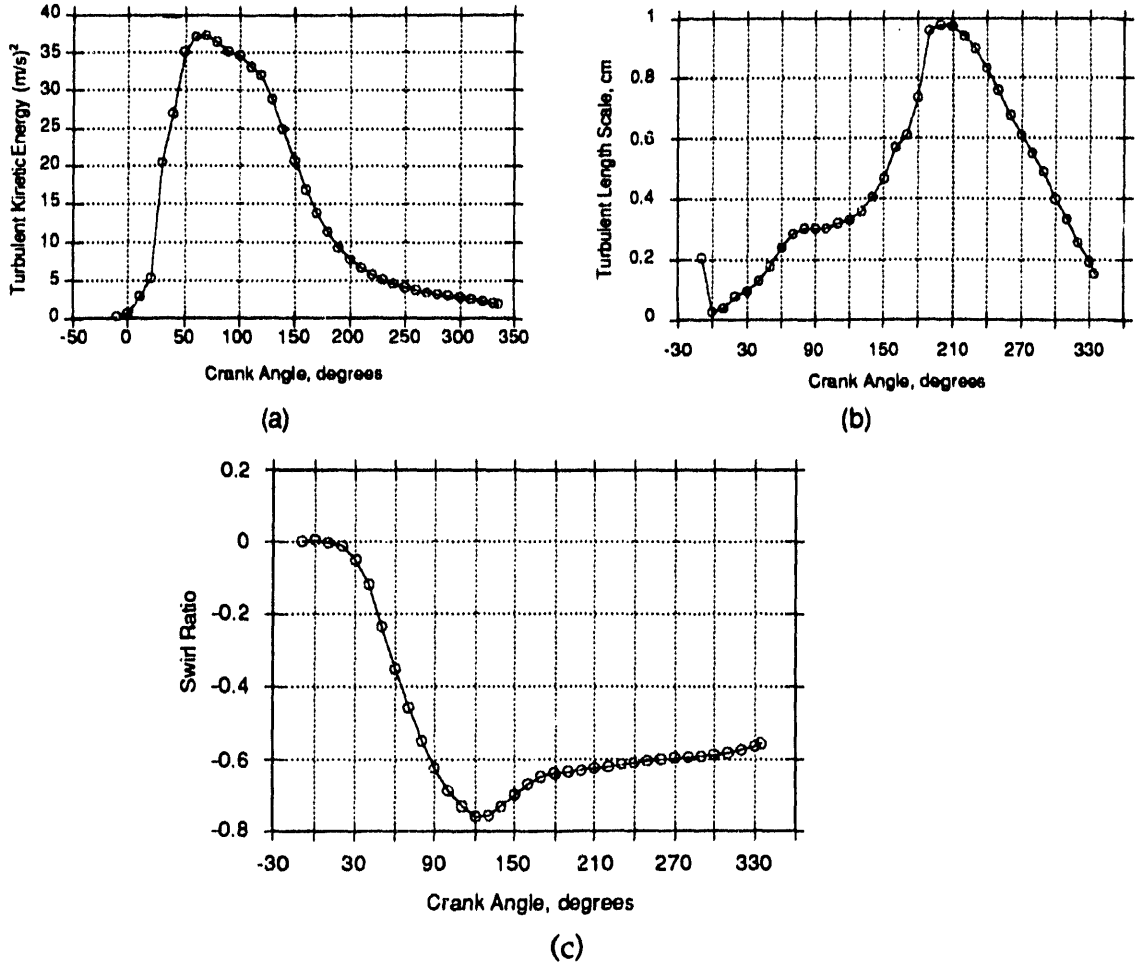

Fig. 13 Volume averaged turbulence intensity (a), length scale (b) and swirl ratio (c) as a function of crank angle during the intake stroke.

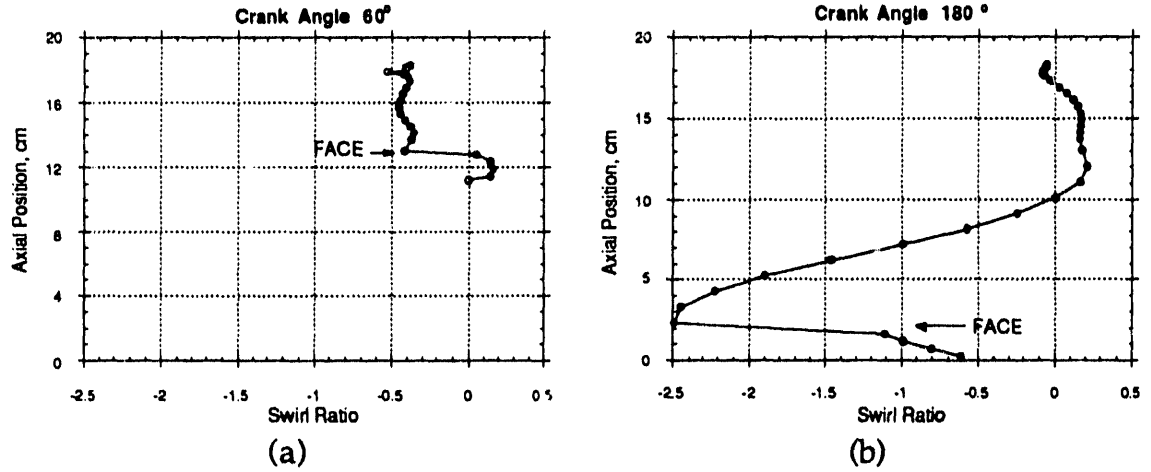

Fig. 14 Swirl ratio variation with depth below the head at (a) 60 and (b) 180 degrees ATDC. The arrow indicates the piston face. Non-zero swirl ratios below the face are in the piston bowl.

Table 5 Swirl magnitudes during intake.

Crank Angle	Peak Swirl Magnitude	Mean Swirl Magnitude	Ratio
180	2.5	0.7	3.6
240	1.4	0.6	2.3
335	0.8	0.55	1.5

cycle continues this opposite swirl diminishes until it is completely gone by the time of injection.

The above results indicate that engines flow fields contain fairly complex structures. In general, the flows were regular and smooth upstream of the valves. Downstream of the valves in the cylinder, the flows progressed from complicated regions with smaller scales to more regular regions with prominent swirl patterns. Simple, global parameters such as swirl or tumble do not adequately describe these flows. The vertical structure of the planar averaged swirl shown in Fig. 14 provides insight into evolution of swirl during the intake and compression processes.

PART B - Model Application

PERFORMANCE TESTS - A preliminary set of performance tests have been conducted on the Caterpillar engine (see PART C - Engine Experiments), and the results have been compared with KIVA predictions. The experiments used the standard Caterpillar pump-line injection system and the experimental conditions were chosen to match data obtained from Caterpillar on a multi-cylinder version of the engine. The experimental conditions are given in Table 6. The results were found to be in good agreement with the multi-cylinder engine data when allowance was made for the increased friction work of the single-cylinder engine.

A diesel engine simulation program was also used to estimate the cylinder wall, valve and piston temperatures, and the simulation was modified to account for the engine geometry, intake and exhaust surge tank volumes, and its heat release model constants were optimized to match the measured in-cylinder pressure trace.

Table 6 Caterpillar Engine Data

Cylinder Bore	137.19 mm
Stroke	165.1 mm
Compression ratio	15.0
Displacement	2.44 liters
Number of spray nozzle orifices	6
Nozzle hole diameter	0.1295 mm
Engine speed	1000 rev/min (constant)
Overall equivalence ratio	0.564
Air flow rate	0.267e-2 kg/cycle
Fuel flow rate	0.883e-3 kg/cycle
Intake tank pressure	124.0 kPa
Intake tank temperature	323 K
Cylinder wall temp	422 K
Cylinder head	586 K
Piston surface	578 K
Valves face	773 K
Mass average gas temperature at IVC	366 K
Cylinder pressure at IVC	133.0 kPa
Swirl number	0.978
Fuel	Tetradecane
Injection starts	23º BTDC
Injection ends	6.85º ATDC

The corresponding predicted and measured cylinder pressure versus crank angle data are shown in Fig. 15. As can be seen, there is good agreement between the experiments and the simulation, and the KIVA computed pressures. It should be noted that the KIVA results were found to be sensitive to grid resolution and the injection details, and the results shown in Fig. 15 used the fine grids recommended by Gonzalez et al. [27], and measured injection duration data.

Work is currently in progress on assessing the accuracy of KIVA predictions of the effect of injection rate and split injections using the experimental data to be described in the next section.

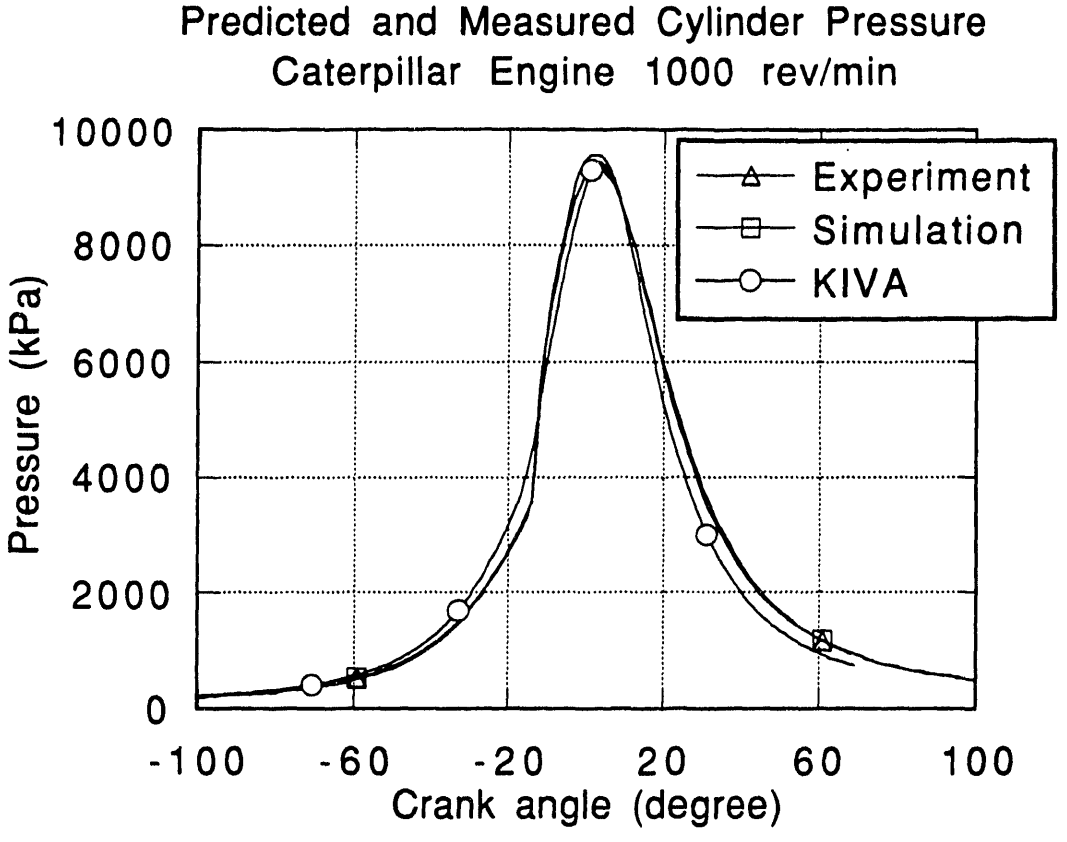

Fig. 15 Comparison between KIVA and (zero-dimensional) engine simulation predictions and the experimental cylinder pressure versus time for the Caterpillar engine at 1000 rev/min.

PART C - Experiments

A supporting experimental program has been initiated to generate data needed for KIVA validations. The engine experiments are conducted using a single cylinder Caterpillar 3406 oil-test research engine. In addition to standard measurements of cylinder gas and fuel pressures, and other measurements, combustion visualization and photography experiments are being made through a window that replaces one of the exhaust valves. In setting up the experiments, effort has been made to ensure that the modifications to the engine for optical access are minimal so that the results will be representative of the actual engine.

The engine has also been equipped with a Nippondenso U2, electronically controlled ultra-high-pressure fuel injector with programmable injection rate shapes and timings, and injection rate data is obtained with a Bosch injection-rate meter.

The experiments are being conducted on a timetable that ensures that data will be available coincident with the model implementation phases of Table 1. Details of progress on the experiments are summarized below.

ENGINE FACILITY - A photograph showing the Caterpillar single cylinder research engine is presented in Fig. 16. An electrical air heater supplies heated, pressurized air (to simulate turbo-charging) to a large volume intake surge tank (partially visible at upper right in Fig. 16). A short-length intake duct with a bell-mouthed entrance leads from the bottom of the intake duct to the engine cylinder head. The exhaust port leads to the insulated exhaust settling chamber (upper left in Fig. 16). Details of the engine geometry are summarized in Table 7.

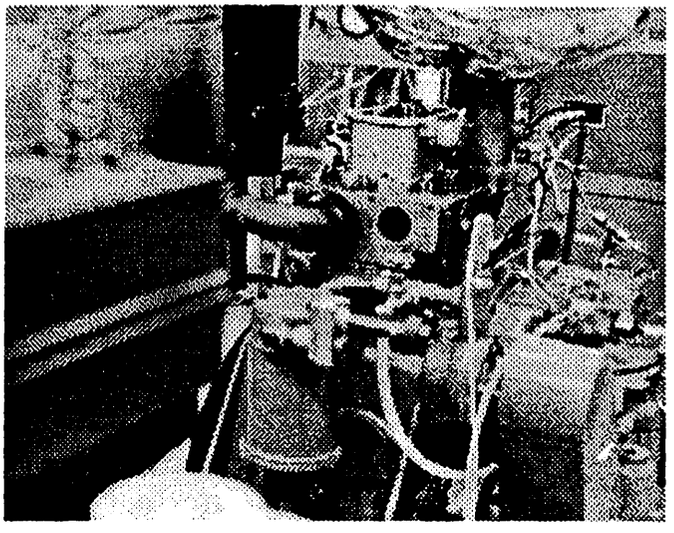

Fig. 16 Photograph of single-cylinder test engine

Table 7 Caterpillar Engine Specifications

Bore		137.19 mm
Stroke		165.1 mm
Connecting Rod Length		261.62 mm
Displacement		2.44 L
Compression Ratio		15
Piston crown		Mexican hat
Engine Speed	up to	2100rev/min
Intake pressure	up to	250 kPa
Intake temperature		up to 450 K
Intake valve close timing		147 deg BTDC
Swirl ratio (nominal)		0.978

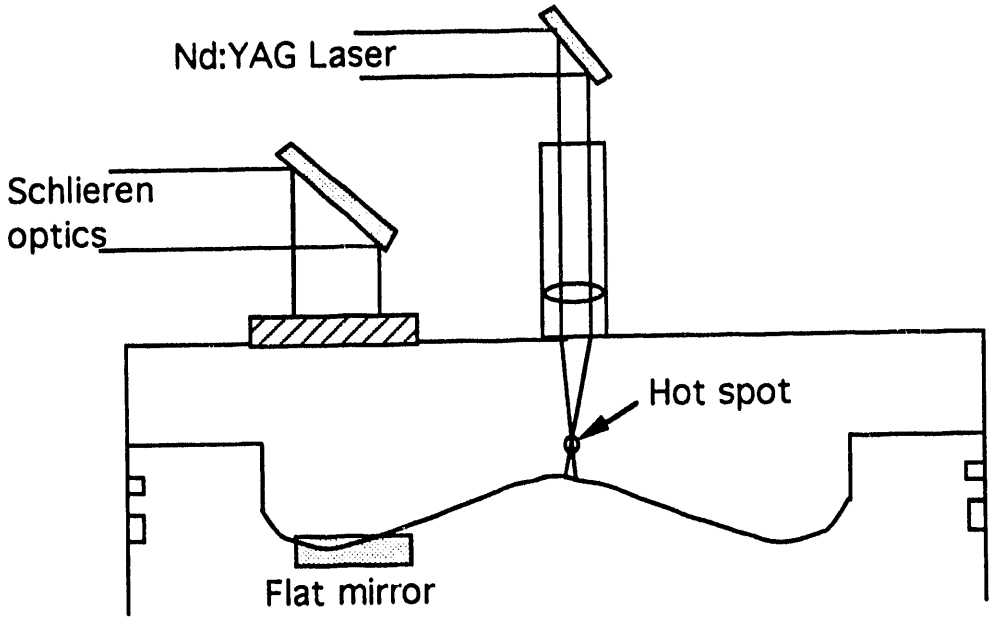

Fig. 17 Optical arrangement for optoacoustic gas temperature measurements.

In Fig. 16, the engine is shown with the cylinder head water cooling removed for motoring engine optical experiments. The Nd:Yag laser (visible at the front left) is being used for in-cylinder velocity and temperature measurements with optical access through a quartz window that takes the place of one of the exhaust valves as indicated in Fig. 17.

A new technique which is based on optoacoustic phenomena has been developed for measuring in-cylinder gas temperature and turbulent diffusivity and is described by Giangregorio et al. [28]. The pulsed laser beam is focused to cause local ionization of air at a point in the combustion

chamber as shown in Fig. 17. This initiates a shock wave and creates a hot spot. The local temperature and turbulent diffusivity are determined by monitoring the shock propagation and the hot spot growth, respectively, with a schlieren photography system.

Measured gas temperatures have been compared with KIVA predictions as shown in Fig. 18 for a motored engine case at 750 rev/min. As can be seen, the agreement is good. The extension of the method for the measurement of turbulence diffusivity is currently in progress.

EMISSIONS MEASUREMENTS - A full dilution emission tunnel has been constructed for the engine experiments. The tunnel allows soot emissions (dry and SOF using Soxhlet extraction) from the engine to be studied as a function of the engine operating conditions. Gaseous emissions are also monitored using a chemiluminescent analyzer for NOx, NDIR for CO/CO2 and a heated Flame Ionization Detector for HC as described by Nehmer [29].

The full-dilution tunnel was designed following EPA recommendations [29], and a schematic diagram of the apparatus is presented in Fig. 19. Sample emissions measurement results are presented in Fig. 20. In this case the engine was operated using the standard oil-test engine pump-line fuel injector for different runs and the results demonstrate the good repeatability of the emissions data.

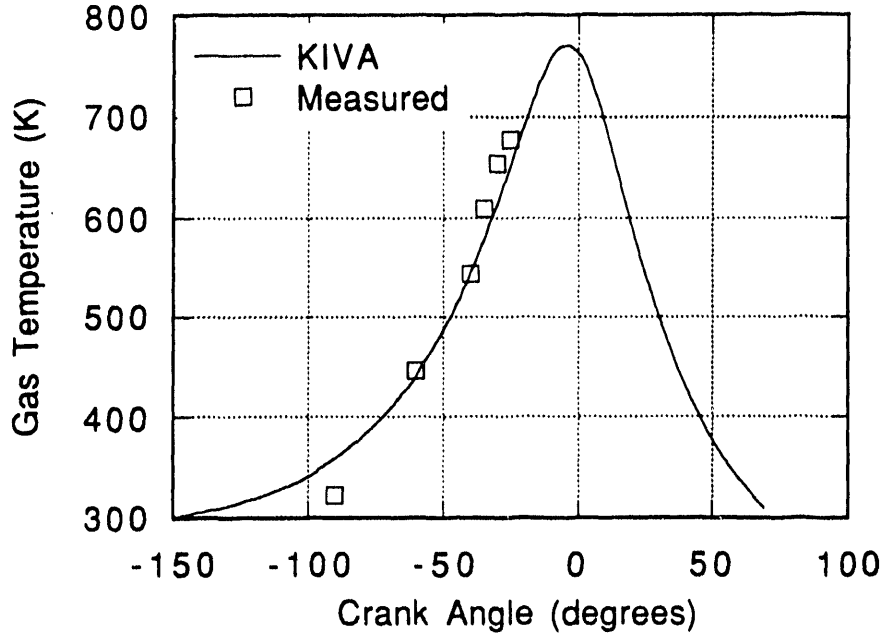

Fig. 18 Measured and KIVA predicted gas temperatures versus crank angle in the Caterpillar engine at a point 12 mm below the head, 25 mm from the axis.

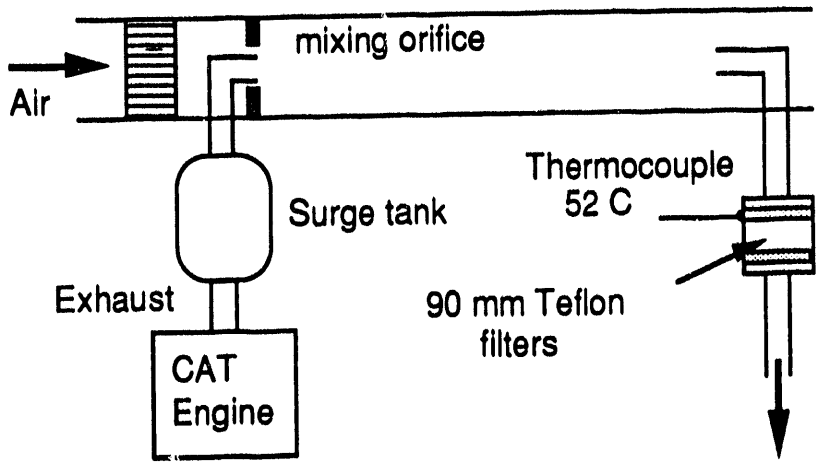

Fig. 19 Schematic diagram of full-dilution tunnel for particulates measurements.

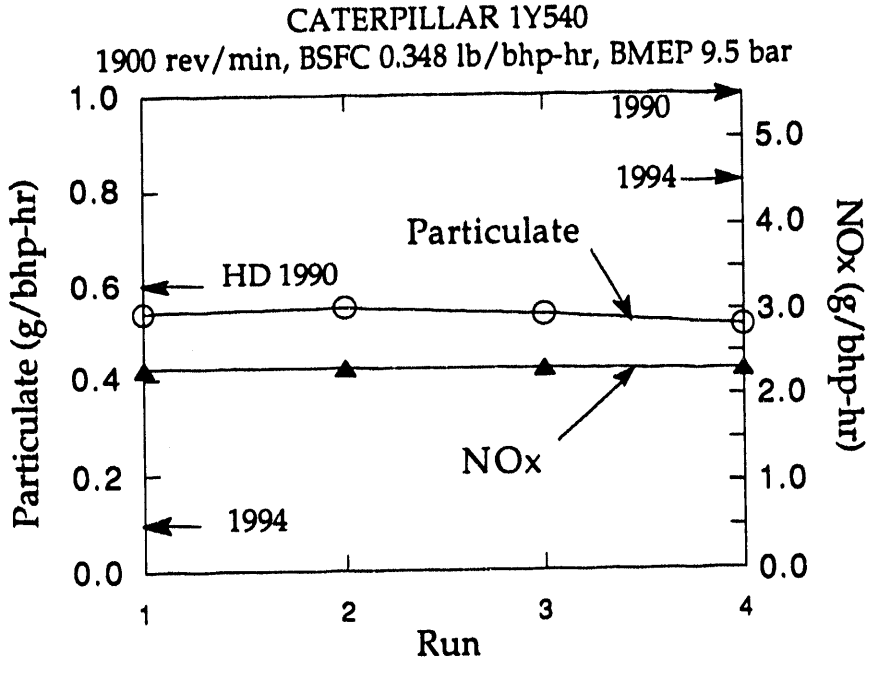

Fig. 20 Particulate and NOx measurements at 1900 rev/min showing repeatability of the emissions measurements for different runs.

The engine experimental data are currently being used to test KIVA's soot and emissions model predictions using the Nippondenso fuel injector with variable rate-shapes and injection timings, including split injections [29].

EFFECT OF INJECTION RATE AND SPLIT INJECTIONS - Electronically controlled diesel fuel injection equipment has been under active development for the past few years. Recent developments in microprocessor technology have created opportunities for better control of fuel delivery and timing than has hitherto been possible. This improved flexibility over the injection parameters offers the possibility of major improvements in diesel engine performance [30]. Improved injection timing flexibility and fast closing times are factors that are known to impact engine emissions [31, 32]. However, the improved flexibility also introduces more configuration possibilities, and this complicates the task of selecting optimum injection parameters. An objective of this research program is to apply advanced modeling techniques to provide guidance for the selection of fuel injection and combustion parameters. This will help in the evolution of more fully optimized, clean and efficient diesel engines.

To help with the model validation effort, experiments are being conducted using the Nippondenso U2 injector system. A schematic diagram of the injector is presented in Fig. 21. The injector features a three-way solenoid valve with an interchangeable check valve for flow control. The initial injection rate can be adjusted by using orifices with different diameter check valves. This is shown in Fig. 22 where check valve orifices of 0.6, 0.3 and 0.2 mm diameter were used to produce injections with rise rates of 2, 7 and 16 crank angle degrees to maximum open (at 1600 rev/min). The injector was operated at 90 MPa (13,230 psia) injection pressure and the nozzle tip features 6 holes with hole diameter of 0.260 mm. The sprays are oriented with the spray axis at an angle of 27.5º to the head. The experimental conditions of the study are given in Table 8 [29].

Table 8. Experimental conditions for Nippondenso injector study

Engine speed	1600 rev/min
Overall equivalence ratio	0.45
Air flow rate	63 g/s
Fuel flow rate	2 g/s
Intake tank pressure	1.82 atm
Intake tank temperature	36 C
Exhaust back pressure	1.57 atm
Injection starts (nominal)*	10º BTDC
Injection ends (nominal)	15º ATDC
3 injection rates	(2º , 7º , 16º to maximum open (0.6, 0.3, 0.2 mm check valve))
4 split injections	(10-90, 25-75, 50-50 and 75-25)
2 different timings between injections	(3º and 8º)

* Injection timing optimized for best BSFC at nominally constant fuel flow

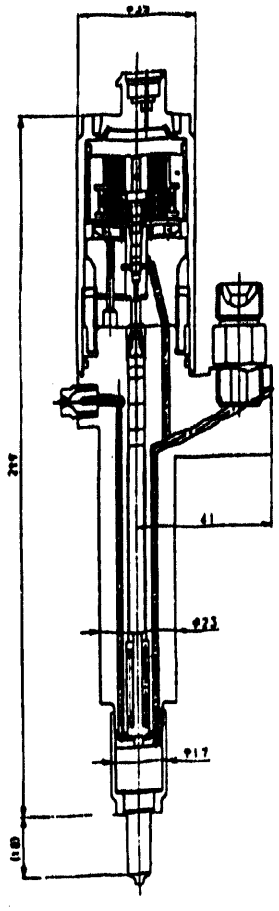

Fig. 21 Schematic diagram of Nippondenso U2 electronic fuel injector. Check valve is located in passage below solenoid.

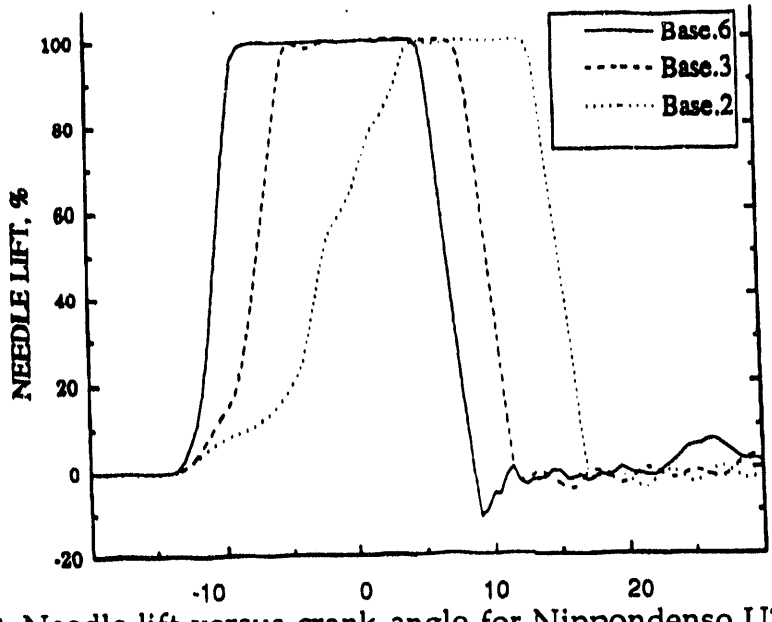

Fig. 22 Needle lift versus crank angle for Nippondenso U2 injector with three different check valve orifice diameters (0.6, 0.3 and 0.2 mm)

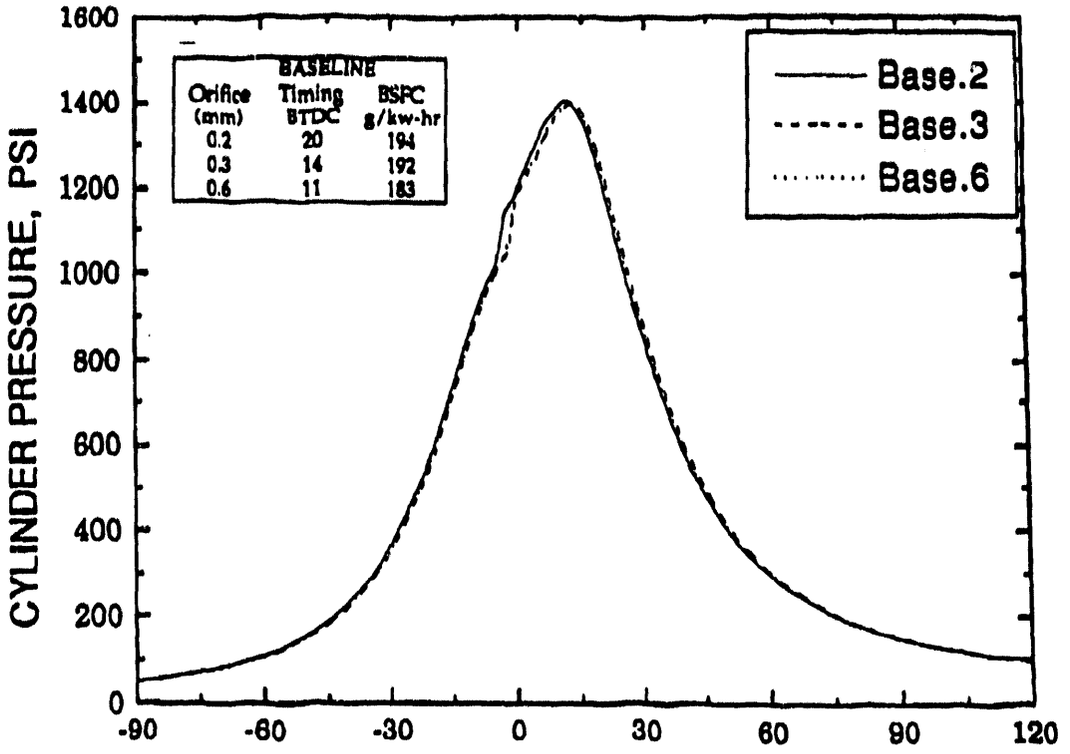

Fig. 23 Measured effect of injection rate on engine cylinder pressure.

The effect of variations in the injection rate on the engine performance is summarized in Fig. 23. As can be seen, the slowest injection rate case (0.2 mm check valve diameter) required the largest injection advance (injection was at 20 degrees before TDC) and the BSFC was 194 g/kw-hr. The best fuel economy was obtained with the fastest rate, 0.6 mm check valve, where the injection was at 11 degrees BTDC and the BSFC was 183 g/kw-hr.

The effect of injection rate on engine soot and NOx emissions is shown in Fig. 24. Comparing the data points labeled 'Base' (open circles) it is seen that the fast injection rate case, Base.6, with the 0.6 mm check valve, gave the lowest NOx and soot levels at about 0.1 and 2.4 g/hp-hr, respectively. These data are within the 1994 heavy duty truck standards, as is indicated in the figure.

The soot (particulate) levels for the slower injection cases, Base.3 and Base.2, are similar to those obtained for the fast rate case, Base.6. However, the data indicates that the NOx levels increase with decreasing injection rate. The low NOx levels associated with the fast injection rate would be explained by the fact that this case also had the shortest ignition delay.

The Soluble Organic Fraction (SOF) data are also given in Fig. 24. It can be seen that the SOF is within 10-15% of the particulate mass, indicating that the test engine is representative of a modern low SOF engine.

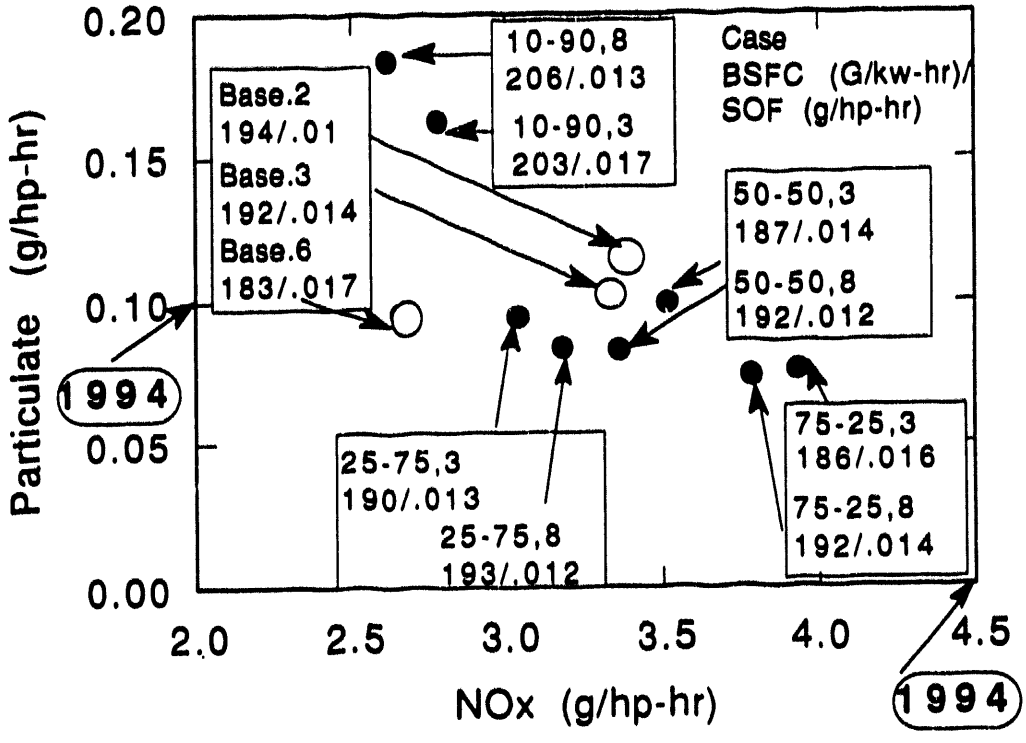

Fig. 24 Measured effect of injection rate (Base.2, .3 and .6) and split injections (10-90, 25-75, 50-50, 75-25% split) on Particulate and NOx emissions (see text).

The effect of split injections on engine performance has also been studied. As indicated in Table 8, split injections were considered with the first injection containing 10, 25, 50 and 75% of the injected mass (and the second injection containing 90, 75, 50 and 25% of the injected mass, respectively). Time periods between the two injections of 3 and 8 crank angle degrees were considered. The corresponding injector needle lift and fuel injection rate data are presented in Fig. 25. As can be seen, the injector affords remarkable control over the details of the injection.

The corresponding measured cylinder pressure data are shown in Fig. 26. Here it is seen that the injection details have a large influence on the combustion process. The injection timing was earlier, and the BSFC increased, as the amount of fuel in the first injection pulse was decreased for both of the spacings between injections considered in the experiments. Figure 24 shows that split injections also influence the engine particulate and NOx emissions significantly. In particular, the soot levels increased as the amount of fuel in the first injection decreased. However, the NOx emissions decreased as the amount of fuel in the first injection was decreased. The effect of the spacing between injections on the emissions is seen to be small.

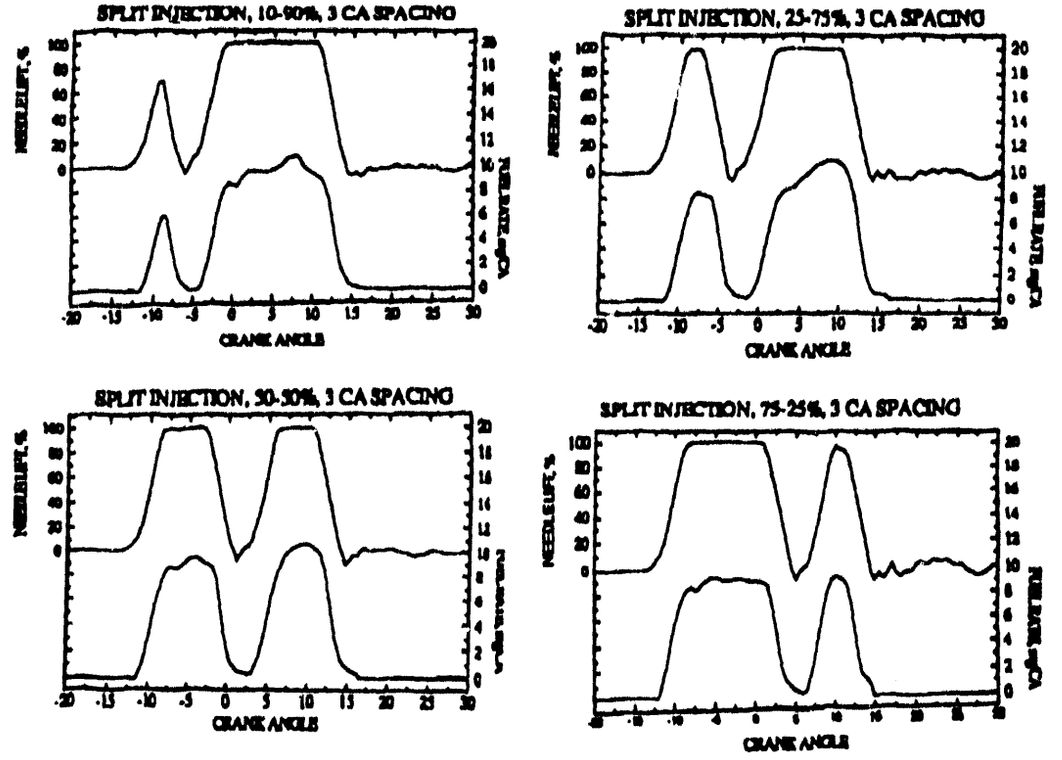

(a)

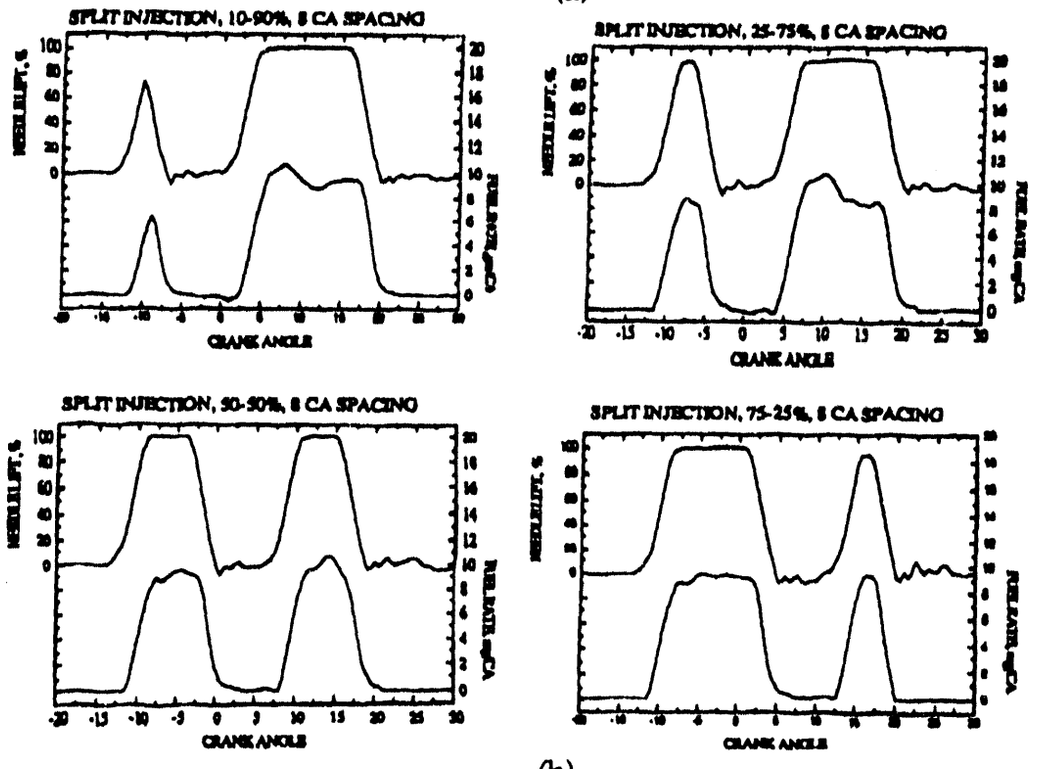

(b)

Fig. 25 Needle lift and fuel flow rate for split injection cases with (a) 3 crank angle degree spacing and (b) 8 degree spacing between injections.

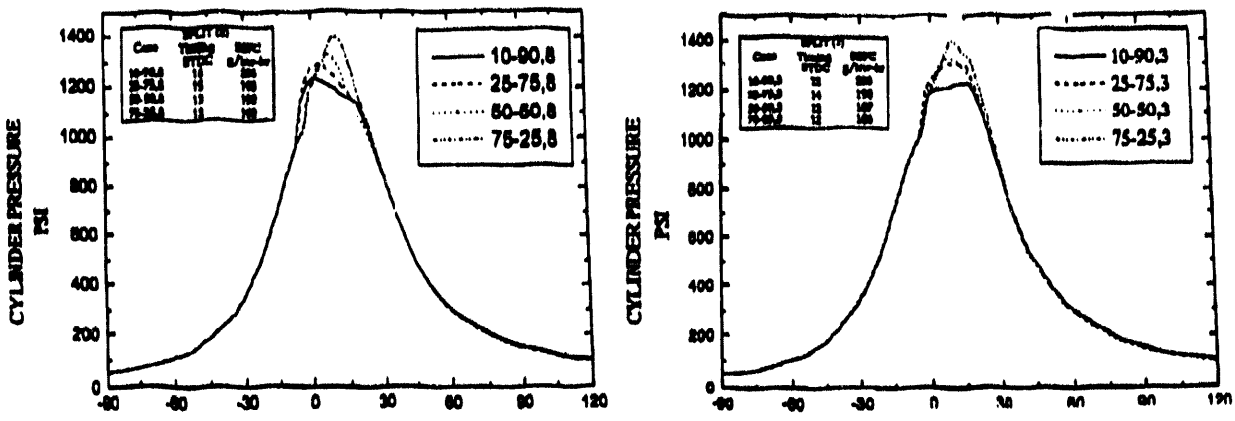

Fig. 26 Measured cylinder pressure data for split injection cases. Left - 8 degree crank angle spacing between split injections, Right - 3 degree spacing.

FLOW VELOCITY MEASUREMENT - Particle Image Velocimetry (PIV) is being used to make gas velocity and turbulence measurements in the (initially) motored engine. PIV provides velocity and turbulence data in a 2-D plane during one realization of the flow (not just at one point as with conventional laser Doppler velocimetry (LDV)). This later feature removes uncertainties associated with the cyclic variability of engine flows that are commonly encountered with single point measurements. The results will be used to validate the KIVA computations of the intake process.

Similar engine modifications to those used for the schlieren temperature and diffusivity measurements will be used for the PIV study. The measurements of gas velocity are made in a plane within the piston bowl using the configuration shown in Fig. 27. A laser sheet is reflected off the central piston cusp which is coated with a reflective coating. A TSI particle seeder is used to supply TiO_2 particles to the intake flow to act as flow markers. A second Q-switch driver (Marx bank) has been installed on the Nd:YAG laser, and the laser is Q-switched twice during the fluorescence lifetime of the flash lamp in a preset time sequence. This produces two images of the TiO2 particles in the plane of the laser sheet on the 35 mm film. The flow velocities are then determined knowing the time-spacing of the images, and by measuring the distance moved by the particles using image analysis techniques.

Preliminary PIV photographic data has already been obtained in a turbulent air jet, and data reduction software has been used to construct the details of the flow velocity field shown in Fig. 28. The details of the turbulent flow structures are clearly visible in the results.

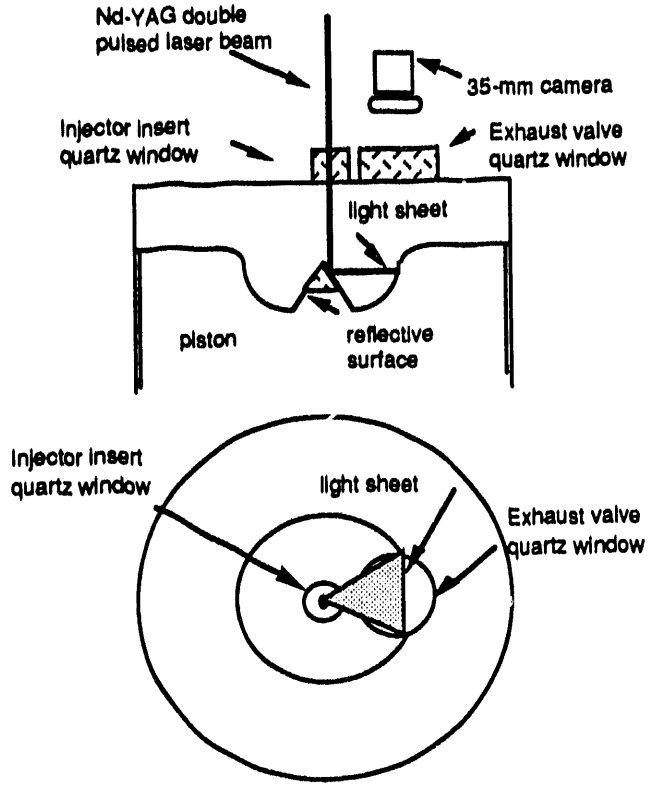

Fig. 27 Schematic diagram of optical layout for in-cylinder PIV.

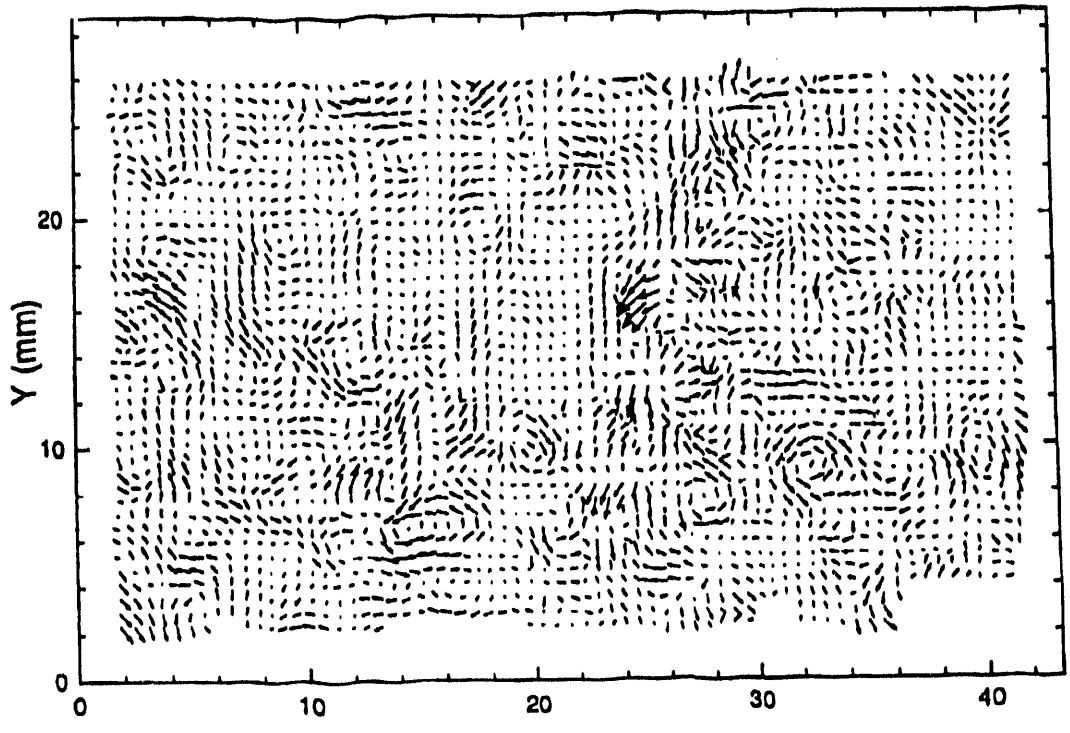

Fig. 28 Velocity vectors in a 2-D plane in a turbulent air jet using PIV.

FUTURE WORK

The research work for the next reporting period will address the entries in Table 1 (page 6) scheduled for year 4: intake flow, vaporization, and soot and radiation. In addition, work will continue on the combustion model and the engine experiments. A major focus will be the application of the model to the conditions of the engine experiments. Details of the individual tasks are described briefly below.

Intake flow modeling

Work on this project is continuing along several lines. First, more detailed experimental data is being obtained to help with validation. Experimental flow visualization, possibly with PIV data, will be used to compare large scale structures. This will help address issues pertaining to the turbulence modeling and grid resolution. Secondly, more unsteady calculations are being made and the flow structure is being examined in more detail. Particle traces and vertical structure of turbulence and other quantities are being obtained. Finally, since the unsteady intake calculations are expensive (over 40 hours of Cray Y-MP time per run), efforts are under way to use the intake flow fields as initial conditions for other calculations. This will provide much better initial conditions for spray and combustion modeling studies.

Multicomponent Fuel Vaporization

The original KIVA vaporization model is a low pressure model that is based on the following assumptions : a. spherical symmetry, b. single component fuel, c. uniform drop temperature, d. constant fuel density and, e. unity Lewis number. Assumptions d. and e. have been removed in the present effort. The preparatory phases of modeling multi-component fuels (assumptions b. and c.) has been completed. The spherical symmetry assumption was considered to be reasonable for stable, non-breaking drops.

Work is continuing on implementing a multi-component fuel vaporization model into KIVA that is based on the works of Refs. [33, 34].

Soot and Radiation

The performance of the Surovkin and Hiroyasu soot models in engine computations will continue to be assessed. It is planned that the radiation model of Chang and Rhee [35] will be adapted for use in this study. This model assumes the Rayleigh-limit for the soot emissivity and a band model for the gas emissivity. More complicated radiation models that require solution of the radiation transport equation and that account for scattering by the spray drops are available [36]. However, in view of the uncertainties about soot concentrations, this additional complexity is not considered to be

warranted at the present time. Much work is being done in this area and it will be monitored for its appropriateness for inclusion in KIVA.

Combustion

As discussed earlier, the present results indicate that the ignition process is well represented by the Shell multi-step kinetics model. However, the results indicate that the single step Arrhenius combustion model is inadequate for the main stage of combustion after ignition. To address this shortcoming the effect of turbulence will be included in the combustion model. This will be accomplished using a Magnussen-Hjertager type model [37] and also the characteristic time model of Kong et al. [12].

Experiments

Engine experiments will be conducted to assess the effect of injection characteristics (injection rate and split injections) on engine performance over a wide range of engine operating conditions. It is planned to include combustion visualization experiments to allow the location and extent of combustion within the combustion chamber to be compared with the model predictions. These experiments will be conducted using a modified version of the engine with one of the exhaust valves replaced by a window for optical access. The PIV measurements of in-cylinder turbulence and velocity distributions will be conducted, and the results compared with the KIVA intake flow predictions.

Model Application

The model will be used to study the influence of engine operating conditions and fuel injection parameters (injection pressure, timing and rate shape - including pilot injection) on in-cylinder fuel-air distributions, combustion and emissions. The model predictions will be validated by comparison with the experimental cylinder pressure and other data.

The rapid pressure rise that can result from premixed combustion of fuel that is vaporized during the ignition delay period has important implications on engine noise and structural loading. Over-mixed vaporized fuel is responsible for the increase in HC emissions found with an increased ignition delay. The influence of the fuel injection parameters on fuel vaporization and mixing during the ignition delay and the early stages of combustion will be studied using the model. Particulates are thought to be formed when under-mixed regions are exposed to high temperatures. The influence of the fuel injection parameters and in-cylinder flow details on mixing and combustion during the main burning phase will also be assessed.

SUMMARY AND CONCLUSIONS

The three-dimensional KIVA code is being modified to include state-of-the-art submodels for diesel engine flow and combustion. Improved and/or new submodels for wall heat transfer with unsteadiness and compressibility, laminar-turbulent characteristic time combustion with unburned HC and Zeldo'vich NOx, spray/wall impingement with rebounding and sliding drops have already been implemented, as described in a previous annual report [5].

The present report describes progress on implementing improved models for spray drop drag and breakup, diesel ignition/combustion and soot formation. The results show that the effect of drop distortion on drop drag needs to be included for accurate spray computations. Also, the drop breakup results indicate that a surface wave breakup model predicts atomization drop sizes more accurately than the standard KIVA oscillating drop breakup (TAB) model. The combustion results indicate that the Shell multistep kinetics model gives accurate predictions of the diesel ignition process. However, further work is needed to assess the effects of turbulence on combustion during the later stages of combustion. The preliminary soot and NOx model results presented here are encouraging, but need further testing by comparison with engine experiments.

A block structured version of KIVA together with an advanced grid generation scheme has been implemented. These codes have been applied to model a realistic engine geometry with steady and moving intake valves. Predicted steady flows agree reasonably with steady-state experimental data, and the moving valve results are encouraging. The accuracy of these results will be tested by comparison with measurements.

An engine test facility has been constructed to allow validation of the in-cylinder flow and soot and NOx emission predictions. A single-cylinder, modern, well characterized research engine that meets the 1994 particulate and NOx emission standards has been setup. The engine's SOF levels were between 10-15 % of the soot mass which is also representative of the values found in modern low emission engines.

The engine has been used to study the effect of injection rate and split injection on engine emissions. It was found that a fast rate of injection gives best overall engine performance with respect to load, soot and NOx emissions. In addition, the results show that a split injection has a large effect on the rate of cylinder pressure rise and the NOx emission is strongly effected by rate of cylinder pressure rise. Increased soot levels are obtained when a small first injection quantity (pilot injection) is used, possibly due to poor spray development, and a shorter interval between split injections improves BSFC. However, the effect of the interval between split injections on soot and

NOx is mixed. These results form a data base for future KIVA validation studies.

An optoacoustic measurement technique has been developed for in-cylinder gas temperature and turbulent diffusivity measurements. Local gas temperature measurements in the motored diesel engine were in good agreement with KIVA model results. Other results in quiescent and turbulent jets indicate that the gas temperature measurements are accurate to within 3%. Work is in progress on improved optical arrangements for engine turbulent diffusivity measurements.

ACKNOWLEDGMENTS

This work was supported under NASA-Lewis grant NAG 3-1087, and the comments of contract monitor W.T. Wintucky are appreciated. Support for the computations was provided by the San Diego Supercomputer Center, Caterpillar and by Cray Research, Inc. The engine and additional support were provided by Caterpillar. The electronic fuel injector was provided by Nippondenso. Additional facilities and support were provided by the Army Research Office contract DAAL03-86-K-0174. The contributions of the many ERC students and staff who made this work possible are also acknowledged.

REFERENCES

1. Amsden, A.A., O'Rourke, P.J. and Butler, T.D., "KIVA-II - A Computer Program for Chemically Reactive Flows with Sprays," Los Alamos National Labs., LA-11560-MS, 1989.
2. Amsden, A.A., O'Rourke, P.J., Butler, T.D., Meintjes, K. and Fansler, T.D. "Comparisons of Computed and Measured Three-Dimensional Velocity Fields in a Motored Two-Stroke Engine," SAE Paper 920418, 1992.
3. Reitz, R.D. and Rutland, C.J."3-D Modeling of Diesel Engine Intake Flow Combustion and Emissions," SAE Paper 911789, SAE Transactions, 1991.
4. Reitz, R.D., Ayoub, N., Gonzalez, M., Hessel, R., Kong, S., Lian, J., Pieper, C., and Rutland, C.J., "Improvements in 3-D Modeling of Diesel Engine Intake Flow and Combustion," SAE Paper 920463, 1992.
5. Reitz, R.D. and Rutland,"3-D Modeling of Diesel Engine Intake Flow Combustion and Emissions," DOE/NASA/1087-1, NASA CR-189126, March 1992.
6. Reitz, R.D.,"Prospects and Challenges for Fuel Spray Research in the Automotive Industry," Atomization and Sprays 2000, NSF Work Proceedings, pp. 89-95, N. Chigier, Ed., Gaithersburg, MD, July 19, 1991.
7. Liu, A.B., Mather, D., and Reitz, R.D., "Effects of Drop Drag and Breakup on Fuel Sprays" SAE Paper 93XXXX, 1993.
8. Liu, A.B. and Reitz, R.D., "Mechanisms of Air-Assisted Liquid Atomization," Atomization and Sprays, Vol. 3, pp. 1-21, 1992
9. Reitz, R.D. "Modeling Atomization Process in High-Pressure Vaporizing Sprays," *Atomisation and Spray Technology* 3 309-337, 1987.
10. O'Rourke, P.J. and Amsden, A.A., "The TAB Method for Numerical Calculation of Spray Droplet Breakup," SAE Paper 872089, 1987.
11. Kong, S.-c., and Reitz, R.D. "Multidimensional Modeling of Diesel Ignition and Combustion Using A Multistep Kinetics Models," ASME Internal Combustion Engine Symposium, Energy-sources Technology Conference and Exhibition, January 31-February 4, 1993, Houston, TX.
12. Kong, S.-C., Ayoub, N., and Reitz, R.D., "Modeling Combustion in Compression Ignition Homogeneous Charge Engines," SAE Paper 920512, 1992.
13. Reitz, R.D. "Assessment of Wall Heat Transfer Models for Premixed-Charge Engine Combustion Computations," SAE Paper 910267, 1991.
14. Kuo, T.-W. and Reitz, R.D. "Computations of Premixed-Charge Combustion in Pancake and Pent-roof Engines," SAE Paper 890670, 1989.
15. Kuo, T.-W. and Reitz, R.D.,"Three-Dimensional Computations of Combustion in Premixed-Charge and Fuel-Injected Two-Stroke Engines, " SAE Paper 920425, 1992.
16. Halstead, M., Kirsh, L. and Quinn, C. "The Autoignition of Hydrocarbon Fuels at High Temperatures and Pressures - Fitting of a Mathematical Model," *Combustion and Flame*, **30**, pp. 45-60, 1977.
17. Theobald, M.A., and Cheng, W.K., "A Numerical Study of Diesel Ignition," ASME Paper 87-FE-2, 1987.

18. Edwards, C.F., Siebers, D.L. and Hoskin, D.H., "A Study of the Autoignition Process of a Diesel Spray via High Speed Visualization," SAE Paper 920108, 1992.
19. Yan, J. and Borman, G.L. "Analysis and in-cylinder measurement of particulate radiant emissions and temperature in a direct injection diesel engine," SAE Paper 881315, 1988.
20. Heywood, J.B.,"Pollutant Formation and Control in Spark-Ignition Engines," Progress in Energy and Combustion Science, Vol. 1, pp. 135-164, 1976.
21. Surovokin, V.F., "Analytical Description of the Processes of Nucleus-formation and Growth of Particles of Carbon Black in the Thermal Decomposition of Aromatic Hydrocarbons in the Gas Phase," Solid Fuel Chemistry, Vol. 10, pp. 92-101, 1976, also in Khimiya Tverdogo Topliva, Vol. 10., No. 1, pp. 111-122, 1976.
22. Gentry, R.A., Daly, B.J. and Amsden, A.A. "KIVA-COAL: A Modified Version of the KIVA Program for Calculating the Combustion Dynamics of a Coal-Water Slurry in a Diesel Engine Cylinder," Los Alamos National Laboratory Report LA-11045-MS, August 1987.
23. Bertoli,C. and P.Belardini, et al; "Three-Dimensional Calculations of DI Diesel Engine Combustion and Comparison with In-Cylinder Sampling Valve Data", SAE Paper 922225, 1992.
24. Nagle, J. Stickland-Constable, R.F., "Oxidation of Carbon between 1000-2000 C," Proc. of the Fifth Carbon Conf., Volume 1, Pergammon Press, p. 154, 1962.
25. Rutland, C.J., Pieper, C., and Hessel, R. "Intake and Cylinder Flow Modeling with a Dual-Valve Port," Accepted for SAE Congress and Exposition, March 1-5, 1993, Detroit, MI.
26. Steinbrenner, J.P., Chawner, J.R. and Fouts, C.L., "The Gridgen 3D Multiple Block Grid Generation System," Flight Dynamics Laboratory Report, Wright-Patterson Air Force Base, WRDC-TR-90-3022, 1990.
27. Gonzalez D., M.A., Lian, Z. W. and Reitz, R.D. "Modeling Diesel Engine Spray Vaporization and Combustion," SAE Paper 920579, 1992.
28. Giangregorio, R.P., Zhu, Y. and Reitz, R.D.,"Application of Schlieren Optical Techniques for the Measurement of Gas Temperature and Turbulent Diffusivity in a Diesel Engine," SAE Paper 93XXXX, 1993.
29. Nehmer, D. MS Thesis University of Wisconsin-Madison, to appear 1993.
30. Glikin, P.E. "Fuel Injection in Diesel Engines," Proceedings of the Institution of Mechanical Engineers, Vol. 199, No. 78, pp. 1-14, 1985.
31. Greeves, G. "Response of Diesel Combustion to Increase in Fuel Injection Rate," Society of Automotive Engineers Technical Paper 790037, 1979.
32. Greeves, G. and Wang, C.H.T. "Origins of Diesel Particulate Mass Emissions," Society of Automotive Engineers Technical Paper 810260, 1981.
33. Jin, J. D., and Borman, G. L., "A Model for Multicomponent Droplet Vaporization at High Ambient Pressures", Society of Automotive Engineers paper 850264, 1985.

34. Abramazon, B., and Sirignano, W. A., "Approximate Theory of a Single Droplet Vaporization in a Convective Field", ASME/JSME Thermal Engineering Conference, Vol. 1, 1987, pp. 11-18.
35. Chang, S.L. and Rhee, K.T. "Computation of Radiation Heat Transfer in Diesel Combustion," Society of Automotive Engineers Paper 831332, 1983.
36. Menguc, M.P., Viskanta, R. and Ferguson, C.R. "Multidimensional modeling of Radiative Heat Transfer in a Diesel Engine," Society of Automotive Engineers Paper 850503, 1985.
37. Magnussen, B.F., and Hjertager, B.H., "On Mathematical Modeling of Turbulent Combustion with Special Emphasis on Soot Formation and Combustion," Sixteenth Symposium (International) on Combustion, pp. 719-729, The Combustion Institute, Pittsburgh, Pa., 1977.

APPENDIX 1_ KIVA USERS GROUP ACTIVITY

The KIVA computer code and its predecessor codes were written at the Los Alamos National Laboratories, New Mexico [1,2]. These codes have seen increasing use by university researchers, government laboratories and engine industries in the U.S. and abroad since the early 1970s. A U.S. KIVA Users group was formed during the DOE Diesel Working Group Meeting at the University of Wisconsin-Madison in the Fall of 1989 . The purpose of this Users Group is to promote the use of KIVA and to facilitate exchange of information among KIVA users. Since that time KIVA Users Groups have also been formed in Europe and Japan.

The U.S. KIVA Users Group currently numbers about 80 organizations. We have served as the editors of the KIVA Users Newsletter and seven issues have already been distributed to the membership (copies of newsletters 5, 6 and 7 are attached in this Appendix). We also co-organized the First and Second International KIVA Users Group Meeting with CRAY Research. These meetings took place in February 1991 and 1992 in Detroit, MI. The meetings were attended by 75 to 80 registrants each. The Third International KIVA Users Group Meeting will take place on February 28, 1993 in Detroit. Details will be released in the 8th KIVA Users Newsletter.

KIVA Users Group Newsletter #5 — November 1991 Editor: Rolf D. Reitz

Users Group Meeting at SAE Congress

Cray Research, Inc. is sponsoring the second International meeting of KIVA Users at the SAE Congress. The meeting is being organized in association with the University of Wisconsin Engine Research Center and will take place at 2:00 pm Sunday, February 23rd, 1992 at COBO-Hall, Detroit, Michigan. This time and place was chosen because it is expected that many KIVA Users will be attending the Society of Automotive Engineers Congress and Exhibition to be held in Detroit, February 24th to 29th.

The meeting will feature about 10 prepared presentations (short descriptions of research in progress) with lively discussions. The presentations will end at about 6:00 pm and will be followed by a Banquet with a Keynote speaker. A registration fee will be collected to help defray the costs of the meal and the facilities. Included in the fee will be a book of abstracts of the presentations which will be distributed to registrants.

If you plan to attend the meeting please contact Reza Taghavi, Cray Research (612) 683-3643 or Rolf Reitz, University of Wisconsin (608) 262-0145 so that we can plan the details of the meeting.

Call for Abstracts

KIVA Users wishing to present their research at the Users Group meeting in Detroit should submit a short abstract (maximum 5 single spaced pages including figures) to Reza Taghavi, Industry, Science & Technology Dept., Cray Research Park, 655E Lone Oak Drive, Eagan, MN 55121 by December 15, 1991. Further details about the abstract and oral presentation formats will be sent to authors later.

European KIVA Users Group Formed

Dr. T. Baritaud (Institut Francais du Petrole, FRANCE) and Professor J. Dent (Loughborough University, ENGLAND) have been active in organizing a European KIVA Users Group. Their first newsletter included a questionnaire to which they have received 23 replies to-date. The majority of users are applying KIVA to study IC engines. Most users indicated that they run KIVA on mainframe computers and that they have also added in-house enhancements to KIVA.

Comparisons of Measured and Calculated Flow Fields in a Motored Two-Stroke Engine using KIVA-3

KIVA-3 computer simulations made at the Los Alamos Laboratories have been compared with measurements of three-dimensional, unsteady scavenging flow in a motored two-stroke engine. As reported at the First International KIVA User's Group Meeting, KIVA-3 differs from KIVA-II in that it uses a block unstructured grid that allows complex geometries to be modeled with significantly greater computational efficiency. For two-stroke engine simulations, KIVA-3 solves the intake and exhaust port flows along with those in the cylinder. Calculating these flows simultaneously is necessary in order to predict the scavenging process accurately.

The experimental measurements were made at General Motors on a modified Suzuki DT-85 crankcase-scavenged engine.[1] Ensemble-averaged velocities were measured, together with the crankcase, exhaust port, and in-cylinder pressures.

Figure 1 is a close-up of the measured and calculated in-cylinder pressures during the time period when the exhaust port is open. Oscillations seen in the calculated cylinder pressure agree well in frequency and amplitude with the experiment. Figure 2 shows a representative comparison at 150 degrees ATDC of measured and calculated velocities. For direct comparison, the calculated velocities are only plotted at the experimental measurement locations. The tumbling motion in the symmetry plane of the cylinder is well replicated by the calculation, and good agreement is shown in planes A and B, which are below the head. The calculations are run for two complete engine revolutions, and the calculated pressures, trapped mass, and velocity fields are nearly the same at 360 and 720 degrees ATDC.

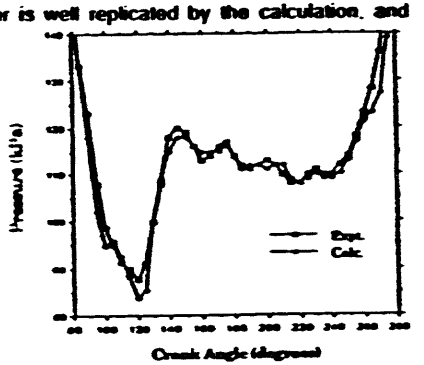

Fig. 1 *Measured and calculated in-cylinder pressures*

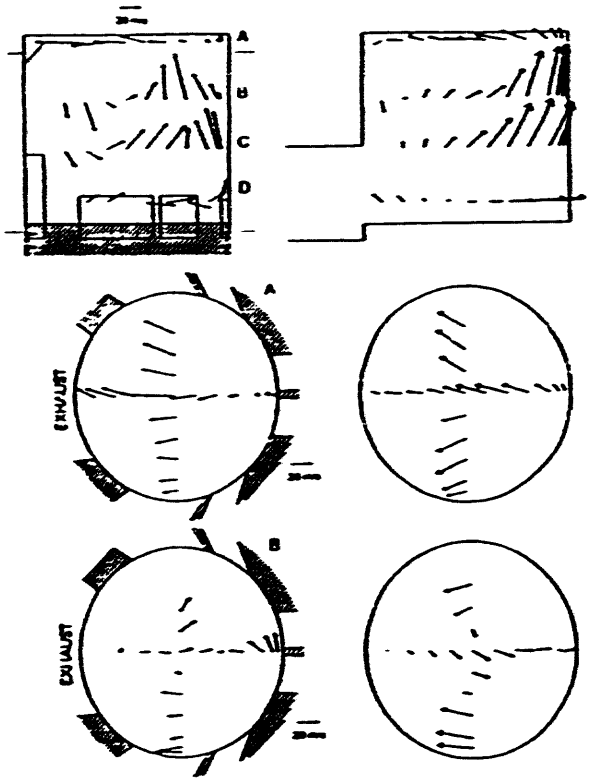

Fig. 2 *Comparison of measured (left) and calculated (right) velocity fields in the two-stroke engine*

The KIVA-3 mesh had 20,729 grid points, and each complete engine revolution required approximately 900 computational cycles and 1.6 hours on a Cray-YMP operating in single processor mode. The comparisons will be presented at the SAE Congress.[2]

[1] T.D. Fansler and D.T. French, SAE Paper 1992.
[2] A.A. Amsden, P.J. O'Rourke, T.D. Butler, K. Meintjes and T.D. Fansler, SAE Paper 1992.

Modeling Diesel Engine Combustion

Diesel engine combustion processes are being studied using KIVA at the University of Wisconsin-Madison. Recent results show that extremely fine numerical grid-spacing is needed to compute vaporizing sprays accurately in high temperature engine environments with combustion.[3] The results shown in Fig. 3 compare spray penetration computations in a Cummins NH engine (made without considering combustion) for two different grids: the first has 25x6x18 cells, with equal spacing in the azimuthal direction; the second has nonuniform azimuthal spacing with increased resolution in the vicinity of the spray - the minimum azimuthal angle is 2 degrees compared to 7.5 degrees in the equally spaced grid. Both grids had 7 axial planes in the bowl and 3 planes in the squish area at TDC. As can be seen, there is a remarkable effect of numerical resolution on the predicted spray penetration. Other results made with even finer meshes suggest that the fine-grid results in Fig. 3 are close to being grid-independent.

Figure 4 shows computations with combustion using the same grids as those used in Fig. 3. The fine grid computation gives a better predicted peak cylinder pressure than the coarse grid computation. However, the predicted pressure still underpredicts the measured pressure. Other results show that the predictions are also sensitive to the details of the combustion and fuel injection models. Thus, further optimization of the results in Fig. 4 requires improved combustion, vaporization and spray models.

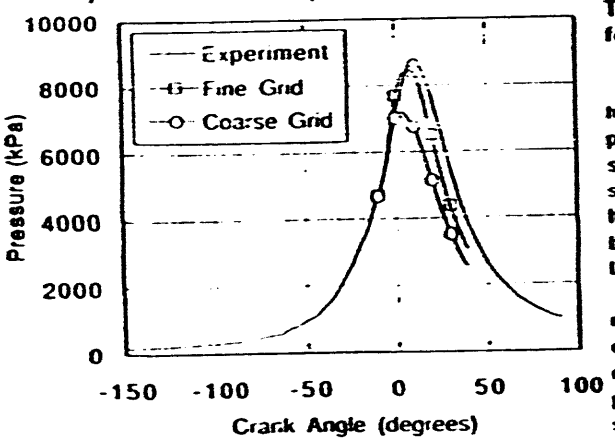

Fig. 4 *Predicted cylinder pressure with combustion showing effect of grid resolution.*

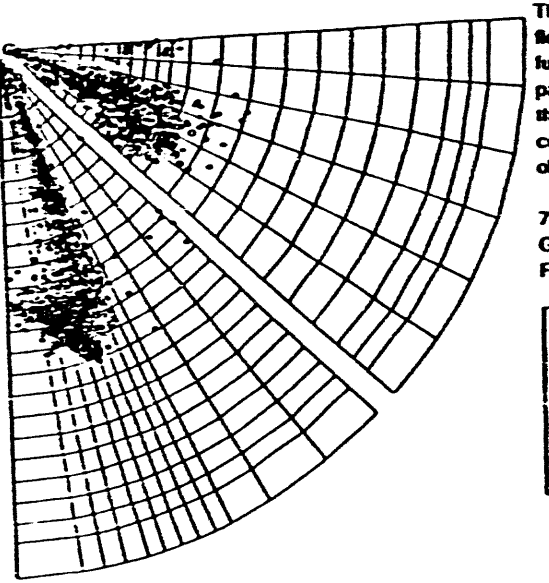

Fig. 3 *Plan view of sprays showing effect of grid resolution on computed spray penetration at TDC (without combustion). Top: Coarse grid. Bottom: Fine grid which uses non-uniform azimuthal spacing.*

[3] M.A. Gonzalez, D., Z.W. Lian and R.D. Reitz, SAE Paper 1992

Three-Dimensional Intake Calculations for a Port-Fuel-Injection Engine

Engines with port-fuel-injection (PFI) systems have become popular as a means of improving vehicle performance through faster response and higher specific output. However, port fuel injection and spray vaporization details influence smoke and hydrocarbon emissions from the engine. KIVA is being used at the General Motors Research Laboratories to analyze the PFI process.

KIVA was modified to account for the effect of a moving valve with a stem using a novel internal obstacle treatment technique in which the valve is represented by a group of discrete computational particles (see Fig. 5). A spray model was used to simulate the fuel injection and the spray model was modified to handle interactions between the spray drops and the valve.

The study demonstrates the importance of the gas flow and fuel injection parameters on the in-cylinder fuel-air mixing process of a PFI engine. In particular, the existence of charge stratification at the time of the spark and the presence of considerable liquid fuel on the chamber walls is observed in the calculations (see Fig. 5).

Further information is available in GMR Report 7406, 1991 by T.-W. Kuo "3-D Port-and-Cylinder Gas Flow and Fuel-Injection Calculations for a Port-Fuel-Injection Engine".

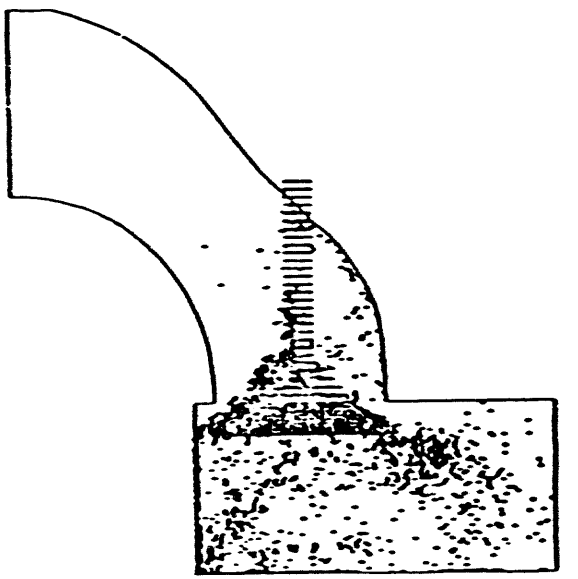

Fig. 5 *Three-dimensional computations of intake port flow and fuel injection. Line-of-sight views of spray parcels in the port and cylinder at 290 degrees BTDC firing with the moving valve represented by discrete computational particles.*

Articles for the Newsletter

Did you like this newsletter? Newsletters will only continue if you submit articles (82% of you polled in the KIVA Users Group Questionnaire said that you would be willing to submit items to our Newsletter!).

For User Group Information please direct correspondence to:
Rolf D. Reitz 123 Engineering Research Building
1500 Johnson Drive University of Wisconsin
Madison, WI 53706 Phone: (608) 262-0145
FAX: (608) 262-6707 reitz@engr.wisc.edu

KIVA Users Group Newsletter #6 --- February 1992 Editor: Rolf D. Reitz

Second International KIVA Users Group Meeting in Detroit at SAE Congress

There is still time to register!

The Second International Meeting of KIVA Users will be held at 2:00 pm Sunday, February 23th, 1992 at the Westin Hotel, Renaissance Center (near COBO-Hall), Detroit, Michigan. This time and place was chosen because it is expected that many KIVA Users will be attending the Society of Automotive Engineers Congress and Exhibition to be held in Detroit, February 24th to 27th.

The meeting is sponsored by CRAY Research and is organized in association with the University of Wisconsin Engine Research Center. The agenda features 9 prepared presentations together with a Keynote address by Dean Hammond of Cray Research. The presentations will be followed by a panel discussion and a social period (cash bar). A registration fee of $15 will be collected to help defray costs, including the book of abstracts of the presentations which will be distributed to registrants.

A Banquet will be held in the Riverfront Ballroom starting at 7:00 pm. The participation fee for those wishing to attend the presentations and the Banquet is $32. The last date for dinner registrations is February 17, 1992 (make checks payable to Cray Research Inc.).

Send advance registration material to Reza Taghavi (Industry, Science and Technology Department, Cray Research Park, 655E Lone Oak Drive, Eagan, MN 55121)

If you plan to attend the meeting please contact Carol Kleinfeld (612) 683-3616 or Reza Taghavi Cray Research (612) 683-3643 for information on registering.

KIVA Users Group Meeting Preliminary Program

Sunday, February 23, 1992
Westin Hotel
Kent Room
Renaissance Center
Detroit, Michigan

Chairman: R. Taghavi, *Cray Research Inc., Eagan, MN, USA*

2:00 Welcome and Announcements

2:15 Grid Size Effects on the Accuracy of Estimating Diffusion and Convection in KIVA-II. K. Kikuta, B. Crary, T. Chikahisa, *Hokkaido University, Sapporo, Japan,* and J.K. Martin, *University of Wisconsin, Madison, WI, USA*

2:35 KIVA-II Modeling of Diesel Spray Experiments in a Combustion Bomb. K.D. Marx, *Sandia Laboratories, Livermore, CA, USA,* and B.C. Dillies, *Laboratoire EM2C du CNRS et de l'ECP, Chatenay-Malabry, FRANCE*

2:55 Parallelization of KIVA-II. B. Gebbeken and C.J. Rutland, *University of Wisconsin, Madison, WI, USA*

3:15 Three Dimensional Port and Cylinder Gas Flow and Fuel Injection Calculations for a Port Fuel Injected Engine. T.-W. Kuo, *General Motors Research Laboratories, Warren, MI, USA*

3:35 Break

3:55 Keynote Address Dean Hammond, Automotive Industry Manager, *Cray Research Inc., Atlanta, Georgia, USA*

4:20 In-Cylinder Flow Measurements by LDA and Numerical Simulation by Kiva Code. P. Belardini, C. Bertoli, F.E. Corcione, *Instituto Motori - CNR, Naples, ITALY*

4:40 Influence of Grid Resolution on Diesel Engine Combustion Predictions, Z.W. Lian and R.D. Reitz, *University of Wisconsin, Madison, WI, USA*

5:00 Three Dimensional Modeling of Fuel Injection, Auto-Ignition and Combustion in an Indirect Injection Diesel Engine, R. Taghavi, *Cray Research Inc., Eagan, MN, USA*

5:20 To be Announced, J.C. Dent and S. Wales *Loughborough University of Technology, Loughborough, ENGLAND*

5:40 3D Multi-Block Structured Version of KIVA-II: First Applications to the Calculation of 2-Stroke Ported Engines, C. Habchi, A. Torres and T. Baritaud, *Institut Francais du Petrole, Rueil-Malmaison, FRANCE*

6:00 Numerical Simulation and Physical Testing: How can Numerical Simulation Help Reduce the Engine Design Cycle Time?,
Panel Discussion open to all Participants

6:30-7:00 Demonstrations, Discussion, Social Period

7:00-9:00 Banquet/Riverfront Ballroom

Selected Short Abstracts of Presentations to be made at the Detroit KIVA Users Group Meeting:

Grid Size Effects on the Accuracy of Estimating Diffusion and Convection in KIVA-II

K. Kikuta, B. Crary, T. Chikahisa, *Hokkaido University, Sapporo, Japan,* and J.K. Martin, *University of Wisconsin, Madison, WI, USA*

Nonphysical diffusion resulting from numerical approximation of gradients must be controlled for accurate computational fluid dynamic simulations, such as those provided by KIVA-II. One method commonly adopted for determining if the grid size is sufficiently small to appropriately approximate spatial gradients is to reduce the grid spacing to a size where further reductions produce little change in calculated quantities. However, KIVA presents unique challenges for such a method because the engine problem is complex, involving complicated geometry, numerous length and time scales, which may require full 3-dimensional simulation to capture the true behavior of the flow, and such difficulties as sprays and combustion. Very few systematic studies have been performed to ensure the diffusional effects are not dominating a result, because this is often not practicable with KIVA, particularly if sprays and combustion are involved. Run times are sufficiently long and expensive that such analysis is not routinely performed. Thus, it seems that a simpler and more accessible method is necessary to determine the accuracy in estimating diffusional effects when using codes such as KIVA.

The approach adopted in this study is to consider numerical errors that arise in the solution of a simplified equation set for a two-dimensional steady-state jet. The equations were nondimensionalized, and similarity was applied, such that the problem could be simplified to be one-dimensional. The equations were then solved numerically using the same numerical schemes as those adopted in KIVA, and the results were compared with the theoretical radial velocity distribution for steady-state jets. The accuracy of the results was investigated using both the quasi-second order upwind (OSOU) differencing and partial donor cell (PDC) differencing.

The results of the study indicate that the numerical grid should be concentrated in regions with steep gradients. It is estimated that, to ensure acceptable accuracy in a three-dimensional simulation of a diesel fuel spray, at least 25,000 nodes may be required (10 in the radial direction, 100 in the azimuthal direction and 25 in the axial direction).

Influence of Grid Resolution on Diesel Engine Combustion Predictions

Z.W. Lian and R.D. Reitz, *University of Wisconsin, Madison, WI, USA*

Diesel engine in-cylinder combustion processes have been studied using the KIVA-II code with particular attention to the influence of numerical errors on combustion predictions. The engine computations were made for a Cummins NH engine for which extensive experimental data are available with measurements of injection characteristics, cylinder pressure, and flame temperatures. Results using a cycle analysis simulation program are also available for the same engine and were used as input for the initial conditions in the multidimensional calculations.

To test the effect of grid resolution on engine combustion predictions, calculations were made using successively finer grids. The computational experiments showed that the results are most sensitive to the azimuthal mesh spacing. This is to be expected since the largest gradients in the flow are across the spray cross-section. Predicted engine cylinder pressures made using meshes with azimuthal mesh spacings of 7.5, 2.25, 1.8 and 1 degrees are shown in Fig. 1 (the computations used 25x18 cells in the radial and axial directions, respectively). It can be seen that finer grid resolution gives higher cylinder pressures. The magnitude of the numerical error in the peak pressure has been estimated using the Richardson extrapolation technique as shown in the Table.

grid $\Delta\phi$	max. pressure (kPa)	error (%)	cpu time (hour)
$\Delta\phi=0$	7233 (est.)	-	-
1°	6875	4.95	14.5
1.8°	6589	8.89	6.5
2.25°	6249	13.6	3.5
7.5°	5619	22.4	0.3

Error estimates for peak cylinder pressure as a function of azimuthal mesh spacing, $\Delta\phi$

As can be seen, the convergence is quite slow, and very fine mesh resolution is needed to get accurate results. The cpu time in the table is the time spent during the combustion period from 18 crank angle degrees before top dead center (BTDC) to 8 degrees after TDC. The results show that to maintain a reasonable accuracy while avoiding excessive computer time, an azimuthal grid size of less than about 2° is a good choice.

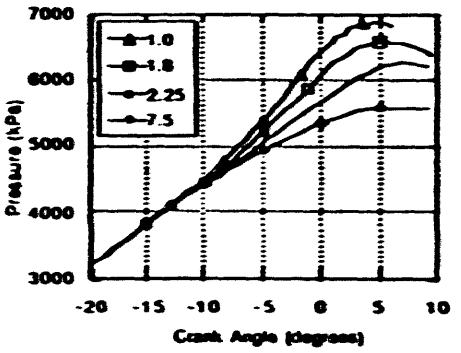

Fig. 1 3-D computations showing effect of grid resolution on predicted cylinder pressures for a Cummins NH diesel engine using grids with azimuthal mesh spacings of 7.5, 2.25, 1.8 and 1.0 degrees (equally spaced mesh).

Articles for the Newsletter

Did you like this newsletter? Newsletters will only continue if you submit articles (82% of you polled in the KIVA Users Group Questionnaire said that you would be willing to submit items to our Newsletter!).

For User Group Information please direct correspondence to:
Rolf D. Reitz 123 Engineering Research Building
1500 Johnson Drive University of Wisconsin
Madison, WI 53706 Phone: (608) 262-0145
FAX: (608) 262-6707 reitz@engr.wisc.edu

KIVA Users Group

Newsletter #7 — June 1992 Editor: Rolf D. Reitz

reitz@engr.wisc.edu FAX: (608) 262-6707

2nd International KIVA Users Group Meeting Held

The 2nd International Meeting of KIVA Users was held on February 23rd, 1992 in Detroit, Michigan. Thanks are due to Cray Research, the sponsors of the meeting. The agenda included 9 presentations with a Keynote address by Dean Hammond of Cray Research.

1993 SAE Congress Session Planned - Use of CFD in Engine Design

An SAE session is being planned by the diesel engine committee for the 1993 International Congress and Exposition in Detroit on the use of Computational Fluid Dynamics as an applied tool. The organizers are interested in papers showing how to use CFD codes such as KIVA in design, rather than papers which discuss code improvements and validations. This topic seems appropriate at this time given the maturity of CFD codes. Abstracts are due by July 27, 1992. Manuscripts are due by October 9, 1992. Interested authors should contact Professor Gary Borman, Engine Research Center, 1500 Johnson Drive ERB, Madison, WI 53706 Phone: (608) 263-1616.

Bibliography of KIVA Publications

Larry Cloutman of the Lawrence Livermore National Laboratory (L^3, MS L-298, Livermore, CA 94551) has proposed compiling a bibliography of KIVA publications that will be maintained under the auspices of the KIVA Users Group. This bibliography will be helpful to both new and veteran KIVA users as a means of contacting other users with expertise in particular application areas. Larry suggests that we only include publications that are obtainable by an average technical library (Journal articles, SAE and AIAA papers, etc.). To have your publications included please send Larry a list of your papers, and/or a listing of other KIVA paper titles that you have found to be useful. FAX: (510) 422-2851.

KIVA-II Simulations of a Richtmyer-Meshkov Instability

Although KIVA was written primarily for application to combustion problems, it can also be used as a general Navier-Stokes solver. Workers at L^3 have recently used KIVA to simulate the Richtmyer-Meshkov (RM) instability. The RM instability is essentially a shock-driven Rayleigh-Taylor instability with the interesting property that the instability occurs regardless of the sign of the density change across the interface separating the two fluids. The RM instability is a prototypical mechanism for turbulent mixing of layered fluids.

KIVA was applied to simulate experiments where a 7.5 cm square shock tube was loaded with helium in the last 8.5 cm of the driven section, and air was the driver gas. The interface between the two gases was given a 2-D single-mode sine wave perturbation shown at cycle 0 in the bottom trace of Fig. 1. An upward traveling Mach 1.24 shock wave sets the interface into motion. The motion consists of two parts - translation up the tube at nearly constant speed, and growth of the sine wave perturbation (see contours at 151ms after shock passage, Fig. 1).

The initial instability is driven by baroclinic production of vorticity generated by the shock wave as it hits the density jump. The total amount of vorticity generated is proportional to the density gradient times the length of time the shock takes to cross the interface thickness. After the shock is reflected from the closed end of the tube, it hits the interface and the translation of the bottom of the interface ceases. However, the instability growth rate increases dramatically and spikes of air move toward the helium end of the tube, see upper trace Fig. 1. At late times the interface shows the same kind of bubble and spike structure typical of Rayleigh-Taylor instabilities, including vortices at the tips of the spikes. This seen in Fig. 1 at t=801 ms.

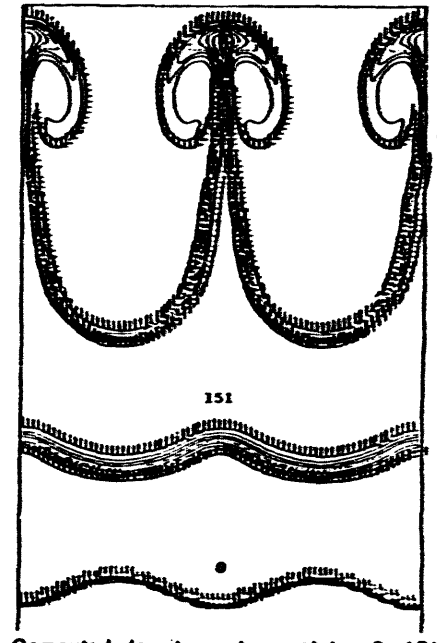

Fig. 1 Computed density contours at t = 0, 151 and 801 ms after passage of the (initially) upward moving shock through the helium (top)/air (bottom) interface.

For more information, contact Larry Cloutman and M. Wehner, Lawrence Livermore Labs, MS L-298, Livermore, CA 94551. Phone: (510) 422-9307.

Massively-parallel Version of KIVA

Los Alamos Labs is working on a version of KIVA for massively parallel computers. This version, called KIVA-CM, is being written in standard FORTRAN-90 and tested on Thinking Machines Inc.'s CM-2 computer. Preliminary comparisons of computational speeds show that KIVA-CM becomes more efficient than KIVA-II as the number of computational cells is increased. This is because inter-processor communication becomes more efficient on the CM-2

as the number of cells is increased. On meshes with greater than about 5,000 cells, KIVA-CM is faster than KIVA-II. In addition to the speed improvement, KIVA-CM will be able to use meshes with as many as a million cells because of the large amount of storage available on the CM-2. KIVA-CM also features improvements to KIVA's numerical solution methods. For more information contact Peter O'Rourke, LANL, Group T-3, Los Alamos, NM 87545. Phone: (505) 667-9091.

Computations of Drop Drag and Breakup

Precise formulation of drop drag and breakup is essential for the accurate modeling of sprays. Comparisons were made using KIVA-II with drop breakup, velocity and trajectory measurements at the University of Wisconsin. The experiments consisted of a Berglund-Liu drop generator and an air jet nozzle, arranged in a cross-flow pattern so that the drops are suddenly exposed to the air, see Fig. 2. Drop sizes were measured with a Phase Doppler Particle Analyzer.

Measured drop trajectories were used to assess the performance of spray breakup models. Drop breakup was modeled using both a wave instability model and KIVA's TAB model. These models contain model constants that were evaluated as part of the study. Figure 3 shows that good agreement with the measured trajectories was found using the parameter AMP0=0 in the TAB model. However, the predicted breakup drop sizes underestimated those of the experiments somewhat. Better agreement with both trajectories and drop sizes was found using the wave breakup model, together with a modified drag coefficient to account for the fact that the parent drops are also deformed by the gas flow as they breakup. Fig. 3 shows good agreement is obtained using the drag coefficient of a distorted sphere, Cd=1.54, rather than the standard sphere value of 0.4. For more information about this study contact the authors: Alex Liu and Rolf Reitz, Department of Mechanical Engineering University of Wisconsin, Madison, WI 53706. Phone: (608) 262-0145.

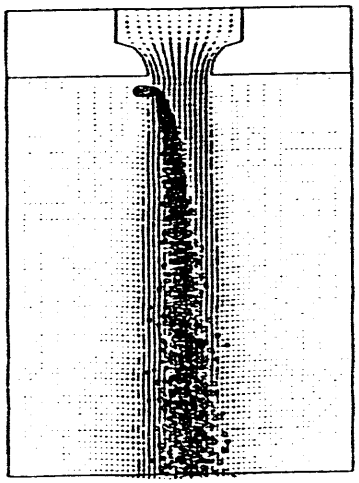

Fig. 2 Computed drop trajectories in the plane of the nozzle. The gas velocity is 100 m/s downwards at the air nozzle exit. 170 μm diameter drops enter the air jet edge at 20 m/s from the left.

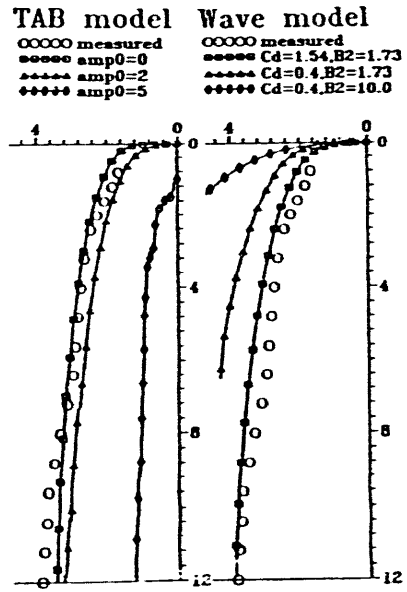

Fig. 3 Measured and predicted (parent) drop trajectories. The drops enter from the upper right and the measured data is indicated by the circles.

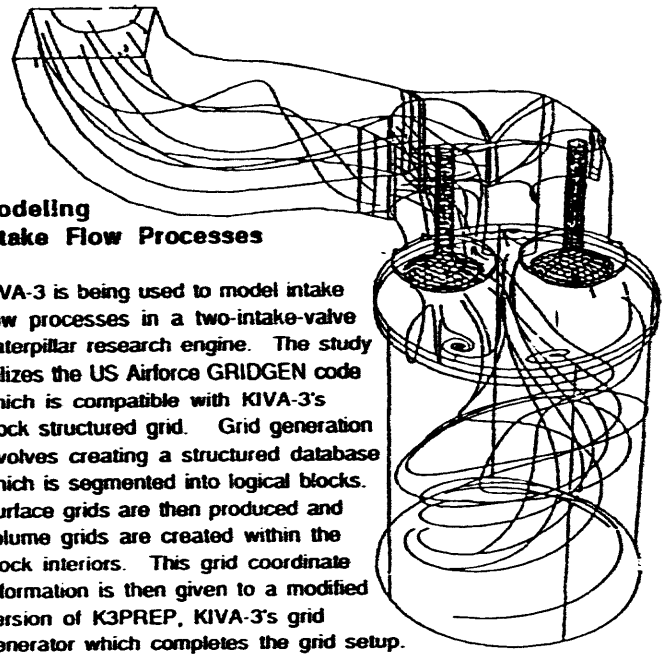

Modeling Intake Flow Processes

KIVA-3 is being used to model intake flow processes in a two-intake-valve Caterpillar research engine. The study utilizes the US Airforce GRIDGEN code which is compatible with KIVA-3's block structured grid. Grid generation involves creating a structured database which is segmented into logical blocks. Surface grids are then produced and volume grids are created within the block interiors. This grid coordinate information is then given to a modified version of K3PREP, KIVA-3's grid generator which completes the grid setup.

Pathlines showing KIVA predictions of the mixing and flow structures that are setup in the cylinder are shown above for a steady flow case (zero rpm). Computations are currently being made that include piston motion and moving intake valves. In this case, an extension of KIVA-3's "snap" algorithm is being implemented to handle the changes in grid connectivity that occur as the valves move. For more information contact C. Pieper, R. Hessel or Chris Rutland, Mechanical Engineering Dept., University of Wisconsin, Madison, WI 53706. Phone: (608) 262-5853.

CRI-TurboKiva

Cray Research Inc., in conjunction with the Los Alamos Labs, has announced the release of CRI-TurboKiva, a version of KIVA-2 that features pre- and post-processors with advanced graphics capabilities. For more information contact Reza Taghavi, Industry, Science and Technology Department, Cray Research Park, 655E Lone Oak Drive, Eagan, MN 55121. Phone: (612) 683-3643.

APPENDIX 2_ LIST OF RELATED PUBLICATIONS AND ABSTRACTS

C. J. Rutland, C. M. Pieper and R. Hessel, "Intake and Cylinder Flow Modeling with a Dual-Valve Port," SAE Congress and Exposition, 1993

Intake port and cylinder flow have been modeled for a dual intake valve diesel engine. A block structured grid was used to represent the complex geometry of the intake port, valves, and cylinder. The calculations were made using a pre-release version of the KIVA-3 code developed at Los Alamos National Laboratories. Both steady flow-bench and unsteady intake calculations were made.

In the flow bench configuration, the valves were stationary in a fully open position and pressure boundary conditions were implemented at the domain inlet and outlet. Detailed structure of the in-cylinder flow field set up by the intake flow was studied. Three dimensional particle trace streamlines reveal a complex flow structure that is not readily described by global parameters such as swirl or tumble. Streamlines constrained to lie in planes normal to the cylinder axis show dual vortical structures, which originated at the valves, merging into a single structure downstream. Initial comparisons of the computational results to data from steady flow-bench experiments are encouraging.

In the unsteady intake calculations, dual moving valves and a piston with a bowl were implemented. Calculations start prior to intake valve opening and end just prior to fuel injection. Velocity vector plots show the characteristic jet like flows from the valve curtain and vortical flow structures in the combustion chamber. Volume averaged turbulent kinetic energy and length, and swirl ratio magnitude increase during intake and decay during compression. The swirl structure is examined and compared to mean values by averaging over horizontal planes.

R.P. Giangregorio, Y. Zhu, R.D. Reitz, "Application of Schlieren Optical Techniques for the Measurement of Gas Temperature and Turbulent Diffusivity in a Diesel Engine," SAE Congress and Exposition, 1993

A new technique which is based on optoacoustic phenomena has been developed for measuring in-cylinder gas temperature and turbulent diffusivity. In the experiments, a high energy Nd:YAG pulsed laser beam was focused to cause local ionization of air at a point in the combustion chamber. This initiates a shock wave and creates a hot spot. The local temperature and turbulent diffusivity are determined by monitoring the shock propagation and the hot spot growth, respectively, with a schlieren photography system.

In order to assess the validity and accuracy of the measurements, the technique was also applied to a turbulent jet. The temperature measurements were found to be accurate to within 3%. Results from the turbulent jet measurements also showed that the growth rate of the hot spot diameter can be used to estimate the turbulent diffusivity.

In-cylinder gas temperature measurements were made in a motored single cylinder Caterpillar diesel engine, modified for optical access. The measured results were in good agreement with those from multidimensional calculations using the KIVA model. However, the presence of density gradients in the gas due to the compression process was found to deteriorate the schlieren images of the hot spot in the engine, and alternative optical arrangements are being explored for engine turbulent diffusivity measurements.

A.B. Liu, D. Mather, and R. D. Reitz, "Modeling the Effects of Drop Drag and Breakup on Fuel Sprays," SAE Congress and Exposition, 1993

Spray models have been evaluated using experimentally measured trajectories and drop sizes of single drops injected into a high relative velocity gas flow. The computations were made using a modified version of the KIVA-2 code. It was found that the drop drag coefficient and the drop breakup time model constant had to be adjusted in order to match the measurements. Based on these findings, a new drop drag submodel is proposed in which the drop drag coefficient changes dynamically with the flow conditions. The model accounts for the effects of drop distortion and oscillation due to the relative motion between the drop and the gas. The value of the drag coefficient varies between the two limits of that of a rigid sphere (no distortion) and that of a disk (maximum distortion). The modified model was also applied to diesel sprays. The results show that the spray tip penetration is relatively insensitive to the value used for the drop drag coefficient. However, the distribution of drop sizes within sprays is influenced by drop drag. This is due to the fact that changes in drop drag produce changes in the drop-gas relative velocity. This, in turn, causes changes in the spray drop size through the drop breakup and coalescence processes. The changes occur in such a way that the net effect on the spray penetration is small over the tested ranges of conditions. These results emphasize that measurements of spray penetration are not sufficient to test and produce improved spray models. Instead, local measurements of drop size and velocity are needed to develop accurate spray models.

R.D. Reitz, N. Ayoub, M. Gonzalez, R. Hessel, S. Kong, J. Lian, C. Pieper and C.J. Rutland, "Improvements in 3-D Modeling of Diesel Engine Intake Flow and Combustion," SAE Paper 921627, 1992

A three-dimensional computer code (KIVA) is being modified to include state-of-the-art submodels for diesel engine flow and combustion: spray atomization, drop breakup/coalescence, multi-component fuel vaporization, spray/wall interaction, ignition and combustion, wall heat transfer, unburned HC and NOx formation, soot and radiation and the intake flow process. Improved and/or new submodels which have been completed are: wall heat transfer with unsteadiness and compressibility, laminar-turbulent characteristic time combustion with unburned HC and Zeldo'vich NOx, and spray/wall impingement with rebounding and sliding drops. Results to date show that: adding the effects of unsteadiness and compressibility improves the accuracy of heat transfer predictions; spray drop rebound can occur from walls at low impingement velocities (e.g., in cold-starting); larger spray drops are formed at the nozzle due to the influence of vaporization on the atomization process; a laminar-and-turbulent characteristic time combustion model has the flexibility to match measured engine combustion data over a wide range of operating conditions; and, finally, the characteristic time combustion model can also be extended to allow predictions of ignition. The accuracy of the predictions is being assessed by comparisons with available measurements. Additional supporting experiments are also described briefly. To date, comparisons have been made with measured engine cylinder pressure and heat flux data for homogeneous charge, spark-ignited and compression-ignited engines, and also initial comparisons for diesel engines. The model results are in good agreement with the experiments.

S.-C. Kong, and R. D. Reitz, "Multidimensional Modeling of Diesel Ignition and Combustion Using A Multistep Kinetics Model," ASME Internal Combustion Engine Symposium, Energy-sources Technology Conference and Exhibition, January 31-February 4, 1993, Houston, TX.

Ignition and combustion mechanisms in diesel engines were studied using the KIVA code, with modifications to the combustion, heat transfer, crevice flow and spray models. A laminar-and-turbulent characteristic-time combustion model that has been used successfully for spark-ignited engine studies, was extended to allow predictions of ignition and combustion in diesel engines. A more accurate prediction of ignition delay was achieved by using a multistep chemical kinetics model. The Shell model was implemented for this purpose and was found to be capable of predicting successfully the autoignition of homogeneous mixtures in a rapid compression machine and diesel spray ignition under engine conditions. The physical significance of the model parameters is discussed and the sensitivity of results to the model constants is assessed. The ignition kinetics model was also applied to simulate the ignition process in a Cummins diesel engine. The post-ignition combustion was simulated using both a single-step Arrhenius kinetics model and also the characteristic-time model to account for the energy release during the mixing-controlled combustion phase. The present model differs from that used in earlier multidimensional computations of diesel ignition in that it also includes state-of-the-art turbulence and spray atomization models. In addition, in this study the model predictions are compared to engine data. It is found that good levels of agreement with the experimental data are obtained using the multistep chemical kinetics model for diesel ignition modeling. However, further study is needed of the effects of turbulent mixing on post-ignition combustion.

APPENDIX 3 FORTRAN SUBROUTINES

The FORTRAN subroutine given in this appendix has been tested for diesel sprays with combustion. The subroutine needs to be compiled and linked together with the standard KIVA subroutines.

Subroutine chem (replaces KIVA subroutine chem)

This subroutine is based on the Ref. [17] Theobald, M.A., and Cheng, W.K., "A Numerical Study of Diesel Ignition," ASME Paper 87-FE-2, 1987 and should be used with Subroutine Chemprn [see Ref. 5].

```
      subroutine chem
c based on

      Theobald, M.A., and Cheng, W.K., "A Numerical Study of Diesel
      Ignition," ASME Paper 87-FE-2, 1987.
c ===========================================================
csong  modified for the use of SHELL autoignition model combined with
c      charateristic-time combustion model which is 'chemprn.f'
c      apply in combustion bomb spray ignition and Cummins NH engine
c
c  (1) species order:   1: fuel     2: O2 3: N2 4: CO2  5: H2O
c                  6: R  7: B  8: Q  9: CO  10: H2
c  (2) in 'itape' set the enthalpy of formation of new species, i.e.,
c      R, B, Q, equal to zero.
c  (3) in 'rinput.f' change the enthalpy of new species, i.e.,
c      R, B, Q, equal to zero.
c  (4) switch  the low-high-temperature chemistry at TCHOP=1000 K
c  (5) the high temperature chemistry refers to the use of the
c      characteristic-time combustion model.
c  (6) species order in previous characteristic-time combustion model
c      has to be changed accordingly.
c ===========================================================
c
c      chem is called by:  kiva
c
c      chem calls the following subroutines and functions:  chemprn
c
c ===========================================================
c
      include 'comd.com'
      COMMON/CHUBS/ICSLOG,ICSLC
      common/hrr/tothrr
      dimension domega(lnrk)
      real kf,kb
      DATA X1,X3,X4 /1. , 0., -1./, Y1,Y3,Y4/0. , 0. , 0.35/
c12h26 dodecane  2d spray
c     DATA FUELN,FUELM,FUELQ,COF,CO2F,PSTOIC,CRATIO,QFUEL,RMN2
c    &/12.,13.,1.92308,.61846,.30462,1.11385,.67,3.9363E12,3.60714/
c14h30 tetradecane  3d Cummins
      DATA FUELN,FUELM,FUELQ,COF,CO2F,PSTOIC,CRATIO,QFUEL,RMN2
     &/14.,15.,1.93333,.62533,.30800,1.12100,.67,3.9363E12,4.10714/
      DATA AF01,EF1,AF02,EF2,AF03,EF3,AF04,EF4
     &/7.3E-4,-7.55E3,180.,-3.53E3,1.47,5.04E3,1.30e6,1.51E4/
      DATA TFREEZ,RTFREZ,TINHIB,CQINH
```

```
     &    /950., 1.052631E-3,1000.,1.E-7/
      DATA AP1,EP1,AP2,EP2,AP3,EP3
     &    /1.E12 , 0.,  1.E11, 7.56E3, 1.E13, 428./
      DATA IGLOG/0/, ICSLOG/0/, IGLOG0/0/, IGLOG2/0/
      DATA TCHOP /1000./
      DATA XSCHEM /1.00/, ICSLIM/200/
c
c <><><><><><><><><><><><><><><><><><><><><><><><><><><><><><><><><><><><><><><><>
c
      tchem=1.0e-10
      icslog=0
      tothr=0.
      do 100 k=1,nz
      i4b=(k-1)*nxpnyp
      do 90 j=1,ny
      i4=i4b+(j-1)*nxp+1
      do 80 i=1,nx
      if(f(i4).eq.0.) go to 80
      if(spd(i4,1).le.0.)spd(i4,1)=1.e-20
      if(spd(i4,2).le.0.)spd(i4,2)=1.e-20
      IF(TEMP(I4).LT.TCUT)GO TO 80
      SISTOC=SIE(I4)
c   DO NOT NEED TO SUBCYCLE IF [B] TOO LOW FOR BRANCHING
      IF(SPD(I4,7)*RMW(7).LE.1.E-15) GO TO 9000
C   DO NOT SUBCYCLE IF CELL TOO HOT FOR AUTOIGNITION EQUATIONS
      IF(TEMP(I4).GT.TCHOP)GO TO 9000
      RTIJK=1./TEMP(I4)
      IF(TEMP(I4).GT.TFREEZ) RTIJK=RTFREZ
      TKBEST=CF(4)*EXP(-EF(4)*RTIJK)
C   TOTAL NET B RATE CONSIDERED TO SET SUBCYCLING
      CONB= SPD(I4,7)*RMW(7)
      CONR= SPD(I4,6)*RMW(6)
      CONQQ= SPD(I4,8)*RMW(8)
      CONRH= SPD(I4,1)*RMW(1)
      CONOX= SPD(I4,2)*RMW(2)
      P1K= AP1*EXP(-EP1*RTIJK)
      P2K= AP2*EXP(-EP2*RTIJK)
      P3K= AP3*EXP(-EP3*RTIJK)
      PTK=1./(1./(CONOX*P1K)+1./P2K + 1./(CONRH*P3K))
      F01=AF01*EXP(-EF1*RTIJK)
      F02=AF02*EXP(-EF2*RTIJK)
      F1L=F01*(CONOX**X1)*(CONRH**Y1)
      F2P=F02*PTK
      TKBEST=ABS((-TKBEST*CONB+F1L*PTK*CONR+F2P*CONR*CONQQ)/CONB)
      ICS=IFIX(DT*TKBEST/XSCHEM)
      if(ics.le.1) ics=1
      IF(ICS.GT.ICSLIM) ICS=ICSLIM
      DTC=DT/(FLOAT(ICS))
      GO TO 9010
 9000 ICS=1
      DTC=DT
 9010 CONTINUE
       IF(ICS.GT.ICSLOG) ICSLC=I4
      IF(ICS.GT.ICSLOG) ICSLOG=ICS
C +++         SET EXPONENTS AND STOICH. COEF. FOR SHELL ....
C             DO NOT MOVE THESE TO A DATA STATEMENT AS THEY ARE
C             OVERWRITTEN IN RINPUT
      FBM(4,2)=CO2F
```

```
      FBM(9,2)=COF
      FBMAM(4,2)=CO2F
      FBMAM(9,2)=COF
      FBM(3,5)=RMN2
      FBM(3,6)=2.*RMN2
      FBMAM(3,5)=RMN2
      FBMAM(3,6)=2.*RMN2
c +++
      DO 75 IC=1,ICS
C     SECOND STAGE IGNITION DETECTOR
      IF((TEMP(I4).GT.1000.).AND.(IGLOG0.EQ.0))GO TO 7002
      GO TO 7003
 7002 WRITE( *,7012) T+(IC-1)*DTC,I4
      IGLOG0=1
 7003 IF((TEMP(I4).GT.1100.).AND.(IGLOG.EQ.0))GO TO 7000
      GO TO 7004
 7000 WRITE( *,7010) T+(IC-1)*DTC,I4
 7010 FORMAT(5X,'1100 DEGREE K IGNITION AT T=',E10.4,' AT CELL ',I5)
      IGLOG=1
 7004 IF((TEMP(I4).GT.2000.).AND.(IGLOG2.EQ.0))GO TO 7006
      GO TO 7020
 7006 WRITE( *,7014) T+(IC-1)*DTC,I4
      IGLOG2=1
 7020 CONTINUE
 7012 FORMAT(5X,'1000 DEGREE K IGNITION AT T=',E10.4,' AT CELL ',I5)
 7014 FORMAT(5X,'2000 DEGREE K IGNITION AT T=',E10.4,' AT CELL ',I5)
      tijk=temp(i4)
      if(tijk.lt.tcut) go to 80
      rtijk=1./tijk
csong
C     FREEZE REACTION RATES OF KNOCK MODEL TO 950 K IF TEMP HIGHER.
C       (NOTE PRE-EXPONENTIAL TEMP FACTOR NOT FROZEN, BUT NEVER USED)
      IF(TIJK.GT.TFREEZ)RTIJK=RTFREZ
      CONQQ=SPD(I4,8)*RMW(8)
C     SHUTDOWN AUTOIGNITION EQUATIONS IF CELL ALREADY HOT.
      IF (TIJK.GT.TCHOP) GO TO 900
      CONOX=SPD(I4,2)*RMW(2)
      CONRH=SPD(I4,1)*RMW(1)
C     JUMP OUT OF LOOP IF NO FUEL OR O2 AVAILABLE
      IF(CONRH.LT.1.E-10) GO TO 76
      IF(CONOX.LT.1.E-10) GO TO 76
      F01=AF01*EXP(-EF1*RTIJK)
      F02=AF02*EXP(-EF2*RTIJK)
      F03=AF03*EXP(-EF3*RTIJK)
      F04=AF04*EXP(-EF4*RTIJK)
      P1K= AP1*EXP(-EP1*RTIJK)
      P2K= AP2*EXP(-EP2*RTIJK)
      P3K= AP3*EXP(-EP3*RTIJK)
      F1L=F01*(CONOX**X1)*(CONRH**Y1)
      F3L=F03*(CONOX**X3)*(CONRH**Y3)
      F4L=F04*(CONOX**X4)*(CONRH**Y4)
       PTK=1./(1./(CONOX*P1K)+1./P2K+1./(CONRH*P3K))
C     ABOVE FORM FOR PTK IS CORRECTED VERSION 11/27/85
      F1P=F1L*PTK
      F2P=F02*PTK
      F3P=F3L*PTK
      F4P=F4L*PTK
C     SPECIAL TEMP/CONC. DEPENDENT STOICHIOMETRY FACTORS
```

```
      EQLL=(F1L*MW(7)+F4L*MW(8))/(MW(1)/FUELM+PSTOIC*MW(2))
      ASP1=(EQLL+1.)/FUELM
      ASP2=(EQLL+1.)*PSTOIC
C     SET STOICH. FACTORS IN PROPAGATION EQUATION NRK=2
      FAM(1,2) = ASP1
      FAM(2,2) = ASP2
      FBM(7,2) = F1L
      FBM(8,2) = F4L
      FBMAM(1,2) = -ASP1
      FBMAM(2,2) = -ASP2
      FBMAM(7,2) = F1L
      FBMAM(8,2) = F4L
      DO 70 IR=1,NRK-1
      rp=1.
      pp=1.
      ne=nelem(ir)
      do 20 kk=1,ne
      isp=cm(kk,ir)
      rom=spd(i4,isp)*rmw(isp)
      if(am(isp,ir).eq.0) go to 10
      if(rom.le.0.) rp=0.
      if(rom.gt.0.) rp=rp*rom**ae(isp,ir)
   10 if(bm(isp,ir).eq.0) go to 20
      if(rom.le.0.) pp=0.
      if(rom.gt.0.) pp=pp*rom**be(isp,ir)
   20 continue
      kb=0.
      kf=0.
      teback=1.
      teford=1.
      ekback=1.
      ekford=1.
   30 if(cf(ir).le.0.) go to 40
c +++
c +++ forward reaction coefficient
c +++
      if(ef(ir).ne.0.) ekford=exp(-ef(ir)*rtijk)
      if(zetaf(ir).ne.0.) teford=tijk**zetaf(ir)
      kf=cf(ir)*teford*ekford
      IF(IR.EQ.2) KF=PTK
      IF(IR.EQ.3) KF=F2P
      IF(IR.EQ.5) KF=F3P
c +++
c +++ if any rate coefficients cannot be put in standard
c +++ form, code them by hand and put them here
c +++
c +++ find the reference species (the one in greatest danger
c +++ of being driven negative)
c +++
   40 omeg=kf*rp-kb*pp
      rmin=0.
      if(omeg.eq.0.) go to 70
      do 50 kk=1,ne
      isp=cm(kk,ir)
      if(spd(i4,isp).le.0.) go to 50
      rom=omeg*fbmam(isp,ir)*mw(isp)/spd(i4,isp)
      if(rom.ge.0.) go to 50
      if(rom.lt.rmin) iref=isp
```

```
      rmin=min(rmin,rom)
   50 continue
      rom=spd(i4,iref)*rmw(iref)
      flam=fam(iref,ir)
      flbm=fbm(iref,ir)
      ctop=flam*kb*pp + flbm*kf*rp
      cbot=flam*kf*rp + flbm*kb*pp
      domega(ir)=rom*dtc*(ctop-cbot)/((rom+dtc*cbot)*(flbm-flam))
      do 60 isp=1,nsp
      spd(i4,isp)=spd(i4,isp)+mw(isp)*fbmam(isp,ir)*domega(ir)
   60 continue
C     HEAT RELEASE ONLY ON PROPAGATION STEP SCALED BY
C          REACTION CONSUMPTION.
      DECHEM = 0.
      IF(IR.EQ.2) DECHEM=QFUEL*(EQLL+1.)*DOMEGA(2)/RO(I4)
      sie(i4)=sie(i4)+dechem
   70 continue
  900 CONTINUE

C     DISALLOW HEAT RELEASE IF T.LT.TINHIB [NEW]
      IF(TIJK.LT.TINHIB)GO TO 970
csong switch to char. time model 071792
      call chemprn(i4)
      spd(i4,6)=1.e-20
      spd(i4,7)=1.e-20
      spd(i4,8)=1.e-20
      go to 970
C     MAIN HEAT RELEASE IR=NRK. LAST KINETIC EQN
      IR=NRK
C          RESET TEMP TO UNFREEZE IF PREVIOUSLY FROZEN
      RTIJK=1./TIJK
      RP=1.
      PP=1.
      NE=NELEM(IR)
      DO 920 KK=1,NE
      ISP=CM(KK,IR)
      ROM=SPD(I4,isp)*RMW(ISP)
      IF(AM(ISP,IR).EQ.0) GO TO 910
      IF(ROM.LE.0.) RP=0.
      IF(ROM.GT.0.) RP=RP*ROM**AE(ISP,IR)
  910 IF(BM(ISP,IR).EQ.0) GO TO 920
      IF(ROM.LE.0.) PP=0.
      IF(ROM.GT.0.) PP=PP*ROM**BE(ISP,IR)
  920 CONTINUE
      KB=0.
      KF=0.
      TEB=1.
      TEF=1.
      EKB=1.
      EKF=1.
      IF(CB(IR).LE.0.) GO TO 930
C     BACKWARD REACTION COEF
      IF(EB(IR).NE.0.) EKB=EXP(-EB(IR)*RTIJK)
      IF(ZETAB(IR).NE.0.) TEB=TIJK**ZETAB(IR)
      KB=CB(IR)*TEB*EKB
  930 IF(CF(IR).LE.0.) GO TO 940
C     FORWARD REACTION COEF
      IF(EF(IR).NE.0.) EKF=EXP(-EF(IR)*RTIJK)
```

```
      IF(ZETAF(IR).NE.0.) TEF=TIJK**ZETAF(IR)
      KF=CF(IR)*TEF*EKF
C     NONSTANDARD RATE COEF GO HERE
C       FIND REF SPECIES
 940  OMEG=KF*RP-KB*PP
      RMIN=0.
      IF (OMEG .EQ. 0.) GO TO 970
      DO 950 KK=1,NE
      ISP=CM(KK,IR)
      IF(SPD(I4,ISP).LE.0.) GO TO 950
      ROM=OMEG*FBMAM(ISP,IR)*MW(ISP)/SPD(I4,ISP)
      IF(ROM.GE.0.) GO TO 950
      IF(ROM.LT.RMIN) IREF=ISP
      RMIN=AMIN1(RMIN,ROM)
 950  CONTINUE
      ROM=SPD(I4,IREF)*RMW(IREF)
      FLAM=FAM(IREF,IR)
      FLBM=FBM(IREF,IR)
      CTOP=FLAM*KB*PP+FLBM*KF*RP
      CBOT=FLAM*KF*RP+FLBM*KB*PP
      DOMEGA(IR)=ROM*DTC*(CTOP-CBOT)/((ROM+DTC*CBOT)*(FLBM-FLAM))
      DO 960 ISP=1,NSP
      SPD(I4,ISP)=SPD(I4,ISP)+MW(ISP)*FBMAM(ISP,IR)*DOMEGA(IR)
 960  CONTINUE
      DECHEM=QR(NRK)*DOMEGA(IR)/RO(I4)
c +++
      DECHK=ABS(DECHEM/SIE(I4))
      SIE(I4)=SIE(I4)+DECHEM
      TCHEM=AMAX1(TCHEM,DECHK)
 970  CONTINUE
      IF(TEMP(I4).GT.5000.) GO TO 8000
      IF(ICS.EQ.1)GO TO 75
 8000 WRITE( *,8110) T,NCYC,I,J,K,I4,TEMP(I4),SIE(I4),IT,CRANK
      stop 7
 8110 FORMAT(' TEMPERATURE OVERFLOW AT T=',E12.5,' CYC',I5,'I=',I3,
     & 'J=',I3,'K=',I3,'I4=',I5/' TEMP=',E12.5,' SIE=',E12.5,
     & 'IT=',I5,' CRANK=',0PF7.2)
 75   CONTINUE
C     END OF SUBCYCLE LOOP ON CHEMISTRY
 76   CONTINUE
      DESIE=ABS((SIE(I4)-SISTOC)/SIE(I4))
      TCHEM=AMAX1(TCHEM,DESIE)
C     END HEAT RELEASE COMPUTATION
      tothr=tothr+(sie(i4)-sistoc)*ro(i4)*vol(i4)
csong end of SHELL subcycling for current i4 at current time step!
   80 i4=i4+1
   90 continue
  100 continue
      tothrr=tothr*1.e-10/dt
      return
      end
```

DATE FILMED

12 / 13 / 93

END